UNIVERSITY OF MINNESOTA

This is to certify that I have examined this copy of a doctoral thesis by

Soo-hyeon Nam

and have found that it is complete and satisfactory in all respects,
and that any and all revisions required by the final
examining committee have been made.

M.B. Voloshin
(Faculty Adviser)

Date

GRADUATE SCHOOL

Radiative Correction, Mixing, and CP Violation in the B Meson System

A THESIS
SUBMITTED TO THE FACULTY OF THE GRADUATE SCHOOL
OF THE UNIVERSITY OF MINNESOTA
BY

Soo-hyeon Nam

IN PARTIAL FULFILLMENT OF THE REQUIREMENTS
FOR THE DEGREE OF
DOCTOR OF PHILOSOPHY

M.B. Voloshin, Adviser

June, 2005

Acknowledgements

I am deeply grateful to a number of people who have helped me during my graduate studies.

First of all, I am very much obliged to my advisor, Professor M.B. Voloshin, for his patience, guidance, and insights. I owe much of my success to him.

For my thesis, I must thank my final defense committee for their favor and helpful feedback on my thesis. Especially, I am very thankful to Professor S. Rudaz for his invaluable advice and assistance.

I am also thankful to many faculty members, instructors, and my friends in Minnesota for their help and hospitality. They played no small role in my academic career.

Finally, I would like to express my heartfelt thanks to my parents, Y.-C. Nam and H.-S. Lee, and my wife, Jeong-Sun, for their endless love and support. I cannot express my appreciation for them enough.

My dissertation research was supported in part by the DOE grant DE-FG02-94ER40823.

Dedication

With all my love to my parents, my wife, and Jehovah.

Soo-hyeon Nam

131 words

Abstract

We study three major aspects in the B meson system in the standard model and its extensions: **QED** radiative corrections, $B\bar{B}$ mixing, and CP asymmetry. We estimate the isospin-violating **QED** radiative corrections to the charged-to-neutral ratios of two different types of decay rates $\Gamma(B^+ \to J/\psi K^+)/\Gamma(B^0 \to J/\psi K^0)$ and $\Gamma(B^+ \to D_S^+ \bar{D}^0)/\Gamma(B^0 \to D_S^+ D^-)$ taking into account the form factors of the mesons based on the vector meson dominance model, and compare them with the results obtained for the point-like mesons. We also evaluate $B\bar{B}$ mixing and CP asymmetries in $B \to J/\psi K_s$ and $B \to \phi K_s$ decays as well as $B^\pm \to \phi K^{(*)\pm}$ decays in general left-right models using the effective Hamiltonian approach without imposing manifest or pseudomanifest left-right symmetry. Based on recent measurements revealing large CP violation, we show that a nonmanifest type model is more favored than a manifest or pseudomanifest type.

Contents

List of Figures

1 Introduction

The main goal of present experiments in B physics is to study CP violation and test the flavor structure of the standard $SU(2)_L \times U(1)$ model (**SM**) where the quark flavor mixing is described by the Cabibbo-Kobayashi-Maskawa (**CKM**) matrix. The **CKM** description of flavor physics has been very successful in describing the known weak interaction phenomena and played a crucial role in the development of the **SM**. In general, the extraction of **CKM** parameters from experiments is not a straightforward task and is plagued by theoretical uncertainties because the **SM** is written in terms of quarks while experiments are performed with hadrons which involve low-energy strong interactions. In the B meson system, however, the hadronic dynamics in non-perturbative regimes can be simplified by virtue of the usual heavy quark expansion since the b-quark is heavy with respect to the Quantum Chromodynamics (**QCD**) scale parameter $\Lambda_{\rm QCD}$, and hadronic uncertainties in B decays can be eliminated or cancel in appropriate observable quantities such as CP violating asymmetry. Furthermore, large CP-violating asymmetries have been found especially in B decay channels with small branching ratios due to the smallness of the corresponding **CKM** matrix elements. This fact drives the need for high statistics experiments with B mesons in order to determine the **SM** parameters and test the model itself with better accuracy.

1.1 B production and isospin violation

Since the discovery of the b-quark at Fermilab in the Υ bound states in 1977, the major features of properties of B mesons have been most extensively studied at the peak of the $\Upsilon(4S)$ resonance at e^+e^- colliders. For a number of measurements,

including the effects of $B^0\bar{B}^0$ mixing and CP violation, a precise knowledge of the B^+B^- to $B^0\bar{B}^0$ production ratio given by

$$R^{+/0} = 1 + \delta R^{+/0} = \frac{\Gamma\left(\Upsilon(4S) \to B^+B^-\right)}{\Gamma\left(\Upsilon(4S) \to B^0\bar{B}^0\right)} \tag{1}$$

is very important. The recent experimental values of $R^{+/0}$ measured by CLEO [1], BABAR [2], and Belle [3] typically range from 1.01 to 1.10, and the latest precise measurement gives $R^{+/0}_{expr} = 1.006 \pm 0.036 \pm 0.031$ [2].[1] The theoretical prediction of the deviation $\delta R^{+/0}$ has been first made by calculating the Coulomb interaction between point-like mesons [5], and reexamined later by considering the effects of the electromagnetic form factors of the mesons and their interaction vertex [6]. The theoretical values of the ratio $R^{+/0}$ estimated so far range from 1.03 to 1.25. As well as the Coulomb interactions, it was also shown that the strong interaction phase in the region of a strong resonance can modify the experimental result of the ratio $R^{+/0}$ near threshold in e^+e^- annihilation [7].

In practice, the measurements of the ratio $R^{+/0}$ use the yields of events for the exclusive processes where the ratio of the decay rates for B^+ and B^0,

$$\frac{\Gamma(B^+ \to X^+)}{\Gamma(B^0 \to X^0)} \equiv 1 + \delta^{+/0}(X), \tag{2}$$

is determined by the isotopic invariance. An example of such isospin-related decays is provided by $B^+ \to J/\psi K^+$ and $B^0 \to J/\psi K^0$ where the deviation $\delta^{+/0}(J/\psi K)$ due to the isospin-violating mass differences between these two decays is about 0.0014. Since this isospin violation is very small and does not exceed the present experimental accuracy, it has been assumed that $\Gamma(B^+ \to J/\psi K^+) = \Gamma(B^0 \to J/\psi K^0)$.

[1] It can also be mentioned that BABAR recently reported their first result of the direct measurement of the branching fraction $\mathcal{B}(e^+e^- \to B^0\bar{B}^0) = 0.487 \pm 0.010(stat) \pm 0.008(sys)$ using partial reconstruction of the decay $\bar{B}^0 \to D^{*+}l^-\bar{\mu}_l$ [4].

In decays of this type, however, there is still an isospin violation due to Quantum Electrodynamics (**QED**) radiative corrections. Given a non-zero deviation $\delta^{+/0}$, the actual value of the production ratio should be corrected to $R^{+/0} = R^{+/0}_{expt}/(1+\delta^{+/0})$. For precision measurement in present and future experiments, it is important to understand the production ratio $R^{+/0}$ of specific exclusive modes with an accuracy of better than 1%. In particular, the decay mode such as $B^0 \to J/\psi K^0$ requires a better understanding due to its great importance in the measurement of CP violation. Hence, the deviation $\delta^{+/0}(X)$ for a specific decay mode needs to be evaluated more carefully.

The isospin violation in $B \to D$ semileptonic decays was discussed earlier in Ref. [8]. In the decays $B^- \to D^0 l\tilde{\nu}$ and $B^0 \to D^+ l\tilde{\nu}$, for example, the kinematic difference due to the isotopic mass splitting of the D mesons in the spectra is not negligible and can amount to a sizeable fraction of 1%, while the difference is compensated in the total decay rate with a much better accuracy as predicted by the heavy quark effective theory (**HQET**). On the other hand, in the nonleptonic decays where isospin violation due to the mass difference between the charged and neutral mesons is expected to be very small, the **QED** corrections may not be negligible and dominantly lead to the ratio of the corresponding decay rates being off unity. In the **SM**, the **QED** corrections usually amount to an α order where α is the fine-structure constant and differ by sizeable amount depending on the final state masses. In section 2, we will explicitly evaluate the **QED** radiative corrections to the ratios of several decay rates in detail.

1.2 *CP* violation and the CKM matrix

Over the last few years, the study of *CP* violation in the B meson system has undergone dramatic development. In the **SM**, the sizes and patterns of *CP* violation in various decay modes are in principle expressed through one complex phase in the **CKM** matrix [9]. But the present experimental results with large *CP* violation effects in the B meson system are not simply explained with this single parameter under the minimal **SM** framework so the model is challenged both experimentally and theoretically [10].

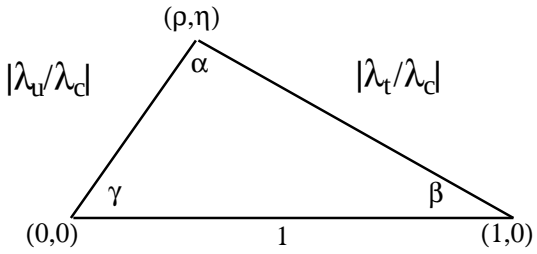

Figure 1: Unitary triangle ($\lambda_i = V_{id}^* V_{ib}$).

Using the Wolfenstein parameterization [11], the **CKM** matrix can be expressed approximately as

$$V = \begin{pmatrix} 1-\lambda^2/2 & \lambda & A\lambda^3(\rho - i\eta) \\ -\lambda & 1-\lambda^2/2 & A\lambda^2 \\ A\lambda^3(1-\rho-i\eta) & -A\lambda^2 & 1 \end{pmatrix} + O(\lambda^4), \qquad (3)$$

where λ (≈ 0.22) is a real expansion parameter, and A, ρ, and η are also real quantities. From the above expression, the elements V_{ub} and V_{td} can be parameterized in terms of two phases γ and β, respectively, which form a unitary triangle (Fig. 1) given by the orthogonality condition $\sum_{i=u,c,t} V_{id} V_{ib}^* = 0$. The *CP* asymmetries in mixing induced B meson decays are characterized by a *CP* angle β, and the

observed world average value of $\sin 2\beta_{expt}$ in $B \to J/\psi K_S$ ($b \to c\bar{c}s$) decays is given by [12]

$$\sin 2\beta_{J/\psi K_S} = 0.731 \pm 0.056. \tag{4}$$

In addition, this CP angle β is recently measured by BABAR and Belle in $B \to \phi K_S$ ($b \to s\bar{s}s$) decays [13],[2] and their average value is

$$\sin 2\beta_{\phi K_S} = -0.39 \pm 0.41. \tag{5}$$

In the **SM**, however, the CP asymmetry in $B \to \phi K_S$ decays is expected to be very close to that in $B \to J/\psi K_S$ decays [15]. While admittedly the error of those experimental data is still too large to confirm the data and justify any theory, a 2.7σ deviation between $\sin 2\beta_{J/\psi K_S}$ and $\sin 2\beta_{\phi K_S}$ may give a clue of new physics (**NP**) effects in B decays. If so, other inclusive $b \to s\bar{s}s$ dominated B decays such as $B^{\pm} \to \phi K^{(*)\pm}$ decays might receive the same contribution from the **NP**, and the experimental value β_{expt} can be expressed through other parameters representing the **NP** as well as the phase of V_{td} in the **SM**.

1.3 $SU(2)_L \times SU(2)_R \times U(1)$ models

As one of the simplest extensions of the **SM** gauge group, and so a complement of the purely left-handed nature of the **SM**, the left-right model (**LRM**) with group $SU(2)_L \times SU(2)_R \times U(1)$ has been widely studied. In this model, even with two generations of quarks one could get CP violation. With three generations of quarks,

[2] At the conference ICHEP2004, both collaborations presented their preliminary results implying $\sin 2\beta_{\phi K_S} = 0.34 \pm 0.20$ which looks closer to the **SM** predictions [14]. However, there is still some room for new physics contributions and we will use their published results given in Eq. (5) for our numerical analysis in this paper.

this model contains many parameters and sources of CP violation [16]. One of the main sources is the relative phase $\alpha_\circ$ between the two vacuum expectation values (VEVs) k and k' of the Higgs bidoublet Φ. The other sources are the complex phases in the left- and right-handed quark mixing matrices V^L and V^R, respectively. Here it would be convenient to regard V^L as the usual **CKM** matrix V and shift all phases except one to V^R. In addition to the phases mentioned above, the masses (M_{W_R}) of the right-handed gauge bosons, the mixing angle ξ between the left- and right-handed gauge bosons W_L and W_R, and the right-handed gauge coupling constant g_R play important roles in **NP** effects as fundamental input parameters in the **LRM**.

The success of the **SM** in the low-energy phenomenology requires that the masses (M_{W_R}) of the right-handed gauge bosons are significantly larger than those (M_{W_L}) of left-handed gauge bosons. The first lower bound on M_{W_R} comes from a study of the low-energy charged current sector allowing $M_{W_R} \gtrsim 3M_{W_L} \approx 240$ GeV [17]. Soon after, many theoretical limits have been presented on M_{W_R} and ξ under various assumptions [18]. The recent experimental limits were obtained by DØ and the collider Detector at Fermilab (CDF) from direct searches for the decay channels of the extra gauge bosons $W'^+ \to \ell_R^+ \nu_R$. DØ found $M_{W'} > 720$ GeV for $m_{\nu_R} \ll M_{W'}$ or $M_{W'} > 650$ GeV for $m_{\nu_R} = M_{W'}/2$ [19]. CDF has the limit of $M_{W'} > 652$ GeV for $m_{\nu_R} \ll M_{W'}$ if ν_R is stable [20]. All of these limits were obtained assuming manifest ($V^R = V^L$) or pseudomanifest ($V^R = V^{L*}K$) left-right symmetry ($g_L = g_R$), where K is a diagonal phase matrix [21]. Nevertheless, we will not impose discrete left-right symmetry which can cause trouble in explaining the cosmological baryon asymmetry and may lead to cosmological domain-wall problems [22]. However, we will also consider the possibility of the left-right symmetric case among other possibilities.

In this paper, we investigate CP violation in the B meson system mainly in

the **LRM** related to the recent experiments. In neutral B decays such as $B \to J/\psi K_S$, the CP asymmetry is governed by $B^0\bar{B}^0$ mixing so that this process has been advocated as a very sensitive probe for CP violation and the presence of right-handed current. The **SM** contribution to $K^0\bar{K}^0$ mixing was previously computed for any internal quark mass by Inami and Lim [23]. The right-handed contribution in the **LRM** was investigated first by Beall, Bander, and Soni, assuming discrete left-right symmetry [24], and again by many authors [25] under various assumptions. But we notice that the contributions of the mixing angle ξ to $B^0\bar{B}^0$ mixing and CP asymmetry can be large due to the heaviness of the top quark mass and the possibility of enhancement in the right-handed quark mixing matrix in the general **LRM**. In addition to $B \to J/\psi K_S$ decays, the CP asymmetry in the penguin-induced $B \to \phi K_S$ decays was also studied earlier in the pseudomanifest left-right symmetry model in Ref. [26]. In this case, the right-handed current contribution to $B^0\bar{B}^0$ mixing is suppressed by the ratio ζ of M_W^2 to $M_{W'}^2$ so that the **NP** effect only arises in the magnetic penguin since the suppression by ξ is offset by a large factor m_t/m_b arising in the virtual top quark loop [27]. However, in the nonmanifest **LRM**, ζ terms in $B^0\bar{B}^0$ mixing and absorptive part of the decay amplitudes become important due to the possible enhancement of V^R elements so that the right-handed current contribution to the corresponding CP asymmetry is more enhanced. In the charged B meson decays such as $B^\pm \to \phi K^{(*)\pm}$ decays, on the other hand, CP violating effects can be observed due to the superposition of CP-odd phases and CP-even phases. After investigating the $B^0\bar{B}^0$ system in the **LRM** in section 3, we will explicitly evaluate the possible right-handed current contribution to CP asymmetries using the effective Hamiltonian approach in several charged and neutral B decays in the general **LRM**, and show that CP asymmetries in those decays can

be large enough to probe the existence of the right-handed current in section 4 in detail.

Before we proceed our discussion on CP violation further, we briefly review here some of the main features of the **LRM**, which are needed to obtain our results. The gauge group of the **LRM** breaks down to that of the **SM** and it finally cascades down to $U(1)_{EM}$. The covariant derivative for the fermions $f_{L,R}$ with respect to the gauge group of the **LRM** appears as

$$D^{\mu} f_{L,R} = \partial^{\mu} f_{L,R} + i g_{L,R} W^{\mu a}_{L,R} T^{a}_{L,R} f_{L,R} + i g_1 B^{\mu} S f_{L,R}. \tag{6}$$

The electric charge which is the unbroken $U(1)$ generator is given by

$$Q = T^3_L + T^3_R + S. \tag{7}$$

The quarks and leptons transform under the gauge group of the **LRM** (T_L, T_R, S) as

$$\begin{aligned} q'_L = \begin{pmatrix} u' \\ d' \end{pmatrix}_L \sim \left(\frac{1}{2}, 0, \frac{1}{6}\right), \qquad q'_R = \begin{pmatrix} u' \\ d' \end{pmatrix}_R \sim \left(0, \frac{1}{2}, \frac{1}{6}\right), \\ l'_L = \begin{pmatrix} \nu' \\ e' \end{pmatrix}_L \sim \left(\frac{1}{2}, 0, -\frac{1}{2}\right), \qquad l'_R = \begin{pmatrix} \nu' \\ e' \end{pmatrix}_R \sim \left(0, \frac{1}{2}, -\frac{1}{2}\right), \end{aligned} \tag{8}$$

where the primes indicate that the fermions are gauge rather than mass eigenstates.

In order to generate masses for the fermions and implement the symmetry breaking, we need to include scalar fields into our theory. The simplest choice is to introduce one Higgs bidoublet Φ and two doublets:

$$\begin{aligned} \Phi = \begin{pmatrix} \phi^0_1 & \phi^+_1 \\ \phi^-_2 & \phi^0_2 \end{pmatrix} \sim \left(\frac{1}{2}, \frac{1^*}{2}, 0\right), \\ \chi_L = \begin{pmatrix} \chi^+ \\ \chi^0 \end{pmatrix}_L \sim \left(\frac{1}{2}, 0, \frac{1}{2}\right), \qquad \chi_R = \begin{pmatrix} \chi^+ \\ \chi^0 \end{pmatrix}_R \sim \left(0, \frac{1}{2}, \frac{1}{2}\right), \end{aligned} \tag{9}$$

which acquire the vacuum expectation values

$$\langle\Phi\rangle = \begin{pmatrix} k & 0 \\ 0 & k' \end{pmatrix}, \quad \langle\chi_L\rangle = \begin{pmatrix} 0 \\ v_L \end{pmatrix}, \quad \langle\chi_R\rangle = \begin{pmatrix} 0 \\ v_R \end{pmatrix}, \tag{10}$$

where k and k' are complex, and v_L and v_R are real. χ_R is needed to generate a large M_{W_R} if $v_R \gg |k|, |k'|, v_L$. But χ_L is not essential unless we impose left-right symmetry. It is also possible to adopt other choices of Higgs field such as Higgs triplets instead [28]. The Lagrangian for the scalar field is

$$\begin{aligned} L_{scalar} &= \mathrm{Tr}[(D^\mu\Phi)^\dagger D_\mu\Phi] + (D^\mu\chi_L)^\dagger D_\mu\chi_L + (D^\mu\chi_R)^\dagger D_\mu\chi_R \\ &\quad - V(\Phi, \chi_L, \chi_R). \end{aligned} \tag{11}$$

For the Higgs fields described above, the kinetic terms in the Lagrangian generate the charged W boson matrix

$$\begin{aligned} M^2_{W^\pm} &= \begin{pmatrix} g_L^2(v_L^2 + K^2)/2 & -g_L g_R k^* k' \\ -g_L g_R k k'^* & g_R^2(v_R^2 + K^2)/2 \end{pmatrix} \\ &\equiv \begin{pmatrix} M^2_{W_L} & M^2_{W_{LR}} e^{i\alpha_\circ} \\ M^2_{W_{LR}} e^{-i\alpha_\circ} & M^2_{W_R} \end{pmatrix}, \end{aligned} \tag{12}$$

where $K^2 = |k|^2 + |k'|^2$ and $\alpha_\circ$ is the phase of k^*k'. After the mass matrix is diagonalized by a unitary transformation the eigenvalues can be expressed in terms of a mixing angle as

$$\begin{aligned} M^2_W &= M^2_{W_L}\cos^2\xi + M^2_{W_R}\sin^2\xi + M^2_{W_{LR}}\sin 2\xi, \\ M^2_{W'} &= M^2_{W_L}\sin^2\xi + M^2_{W_R}\cos^2\xi - M^2_{W_{LR}}\sin 2\xi. \end{aligned} \tag{13}$$

Thus the mass eigenstates are written as

$$\begin{pmatrix} W^+ \\ W'^+ \end{pmatrix} = \begin{pmatrix} \cos\xi & e^{-i\alpha_\circ}\sin\xi \\ -\sin\xi & e^{-i\alpha_\circ}\cos\xi \end{pmatrix} \begin{pmatrix} W_L^+ \\ W_R^+ \end{pmatrix}, \tag{14}$$

where ξ is a mixing angle defined by

$$\tan 2\xi = -\frac{2M^2_{W_{LR}}}{M^2_{W_R} - M^2_{W_L}} \ . \tag{15}$$

For $v_R \gg |k|, |k'|, v_L$, the mass eigenvalues and the mixing angle reduce to

$$M_W^2 \approx \frac{1}{2}g_L^2(v_L^2 + K^2), \quad M_{W'}^2 \approx \frac{1}{2}g_R^2 v_R^2, \quad \xi \approx \frac{2g_L|k^* k'|}{g_R v_R^2}. \tag{16}$$

Here, the Schwarz inequality requires that $\zeta_g \equiv g_R^2 M_W^2/g_L^2 M_{W'}^2 \geq \xi_g \equiv (g_R/g_L)\xi$. From the limits on deviations of muon decay parameters from the V-A prediction, the lower bound on $M_{W'}$ can be obtained as follows [29]:

$$\zeta_g < 0.033 \qquad \text{or} \qquad M_{W'} > (g_R/g_L) \times 440 \text{ GeV}. \tag{17}$$

We will use this number for our numerical analysis.

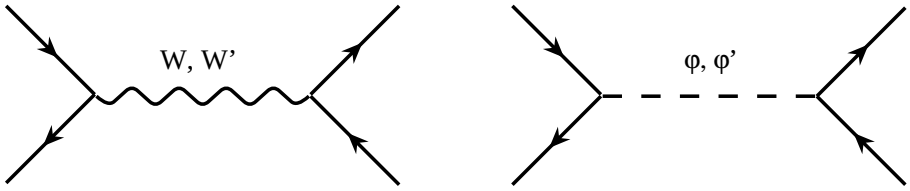

Figure 2: Tree-level Feynman diagrams for the gauge boson (W, W') and the unphysical scalar bosons (φ, φ') exchange.

As well as the above charged gauge bosons, the charged unphysical scalar bosons corresponding to the longitudinal components of the physical bosons take part in the charged current interactions. The coupling of the unphysical scalar fields to the fermions can be found from the detailed structure of the Higgs potential $V(\Phi, \chi_L, \chi_R)$

and the Yukawa couplings. However one can directly determine the unphysical scalar couplings in terms of the gauge couplings without considering the Higgs potential, but using the Ward identities which ensure that the unphysical poles in the two diagrams shown in Fig. 2 should cancel each other [30]. The charged interaction Lagrangian is then given by

$$\begin{aligned} L_{CC} &= -\frac{1}{\sqrt{2}}\overline{P}\gamma^{\mu}\Bigg\{[U^{L}g_{L}c_{\xi}L+U^{R}g_{R}s_{\xi}^{+}R]W_{\mu}^{+}+[-U^{L}g_{L}s_{\xi}L+U^{R}g_{R}c_{\xi}^{+}R]W_{\mu}^{\prime+} \\ &\quad +[(U^{L}M_{P}g_{L}c_{\xi}-U^{R}M_{N}g_{R}s_{\xi}^{+})L+(-U^{L}M_{N}g_{L}c_{\xi}+U^{R}M_{P}g_{R}s_{\xi}^{+})R]\frac{\varphi_{\mu}^{+}}{M_{W}} \\ &\quad -[(U^{L}M_{P}g_{L}s_{\xi}+U^{R}M_{N}g_{R}c_{\xi}^{+})L-(U^{L}M_{N}g_{L}s_{\xi}+U^{R}M_{P}g_{R}c_{\xi}^{+})R]\frac{\varphi_{\mu}^{\prime+}}{M_{W^{\prime}}}\Bigg\}N \\ &\quad +\text{H.c.}+\ldots, \end{aligned} \tag{18}$$

where c_{ξ} (s_{ξ}) $\equiv \cos\xi$ ($\sin\xi$), $s_{\xi}^{\pm} \equiv e^{\pm\alpha_{\circ}}\sin\xi$, $L, R \equiv (1\mp\gamma^{5})/2$ denote left- and right-handed projection operators, $M_{P} = \text{diag}(m_{u}, m_{c}, m_{t})$ and $M_{N} = \text{diag}(m_{d}, m_{s}, m_{b})$ are the diagonalized quark mass matrices, P (N) is the mass eigenstate corresponding to its eigenvalue M_{P} (M_{N}), and U^{L} (U^{R}) is the left- (right-) handed quark mixing matrix. In a similar way to the charged gauge bosons, the neutral gauge bosons mix each other [31]. But we do not present them here because their contributions to $B\bar{B}$ mixing and CP asymmetries in the corresponding B decays are negligible.

2 QED corrections to isospin-related decay rates of B mesons

2.1 Electromagnetic form factors of mesons

In this section, we mainly concentrate on the two different types of the non-leptonic B decays, $B^+ \to J/\psi K^+$ and $B^0 \to J/\psi K^0$ (VP type) decays as well as $B^+ \to D_S^+ \bar{D}^0$ and $B^0 \to D_S^+ D^-$ (PP type) decays where $P(V)$ denotes a pseudoscalar(vector) meson. The calculation of the **QED** radiative corrections due to virtual- and real-photon in the leading order for point-like charged scalar particles is quite straightforward. The radiative corrections due to virtual-photons can be obtained by performing the loop integrals shown in Fig. 3 and Fig. 4.

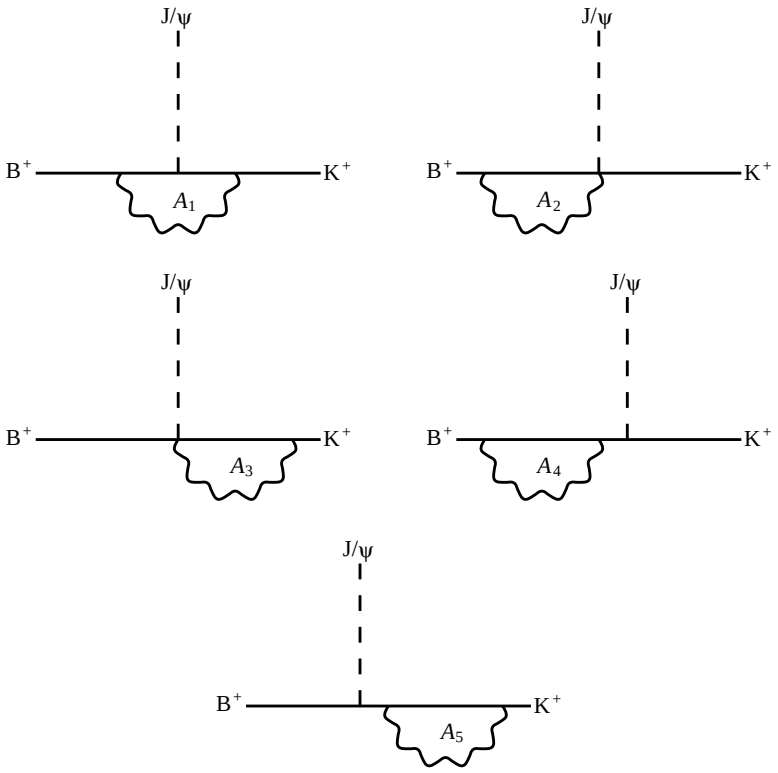

Figure 3: One-loop diagrams for $B^+ \to J/\psi K^+$ decays.

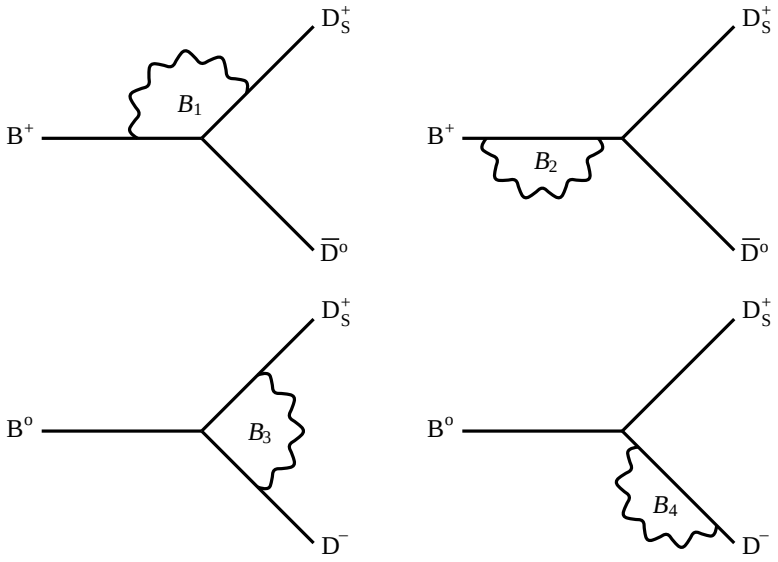

Figure 4: One-loop diagrams for $B^+ \to D_S^+ \bar{D}^0$ and $B^0 \to D_S^+ D^-$ decays. The D_S^+ self-energy makes no contribution to the ratio of the corresponding decay rates.

However, one cannot simply treat the mesons as point-like particles because the **QED** corrections are sensitive to the structure of the mesons, and thus we require models for the form factors of mesons. The electromagnetic form factor F_X of a meson X is successfully modeled in the intermediate energy region using the vector meson dominance model (**VMDM**) [32]. The most commonly used **VMDM** assumes that all photon-hadron coupling is mediated by vector mesons and the form factors are expressed through their propagators. Taking account of the electric charges of the quarks comprising the mesons, we use the **VMDM** based parametrization for the form factors in such a way that each meson behaves like a point-like particle in a zero photon momentum limit as follows:[3]

[3]We assume here that the form factors are primarily associated with the ρ and ω mesons, and neglect the ϕ meson contributions for simplicity, which does not change our result significantly. In other words, we take into account the form factors for the electromagnetic current of the u and d quarks $(2/3)\bar{u}\gamma_\mu u - (1/3)\bar{d}\gamma_\mu d$, and treat the current of the s, c, and b quarks as having a point-like form factor.

$$
\begin{aligned}
F_{B^+}(k^2) &\simeq \frac{1}{3}+\frac{2}{3}\frac{m_\rho^2}{m_\rho^2-k^2} \\
&\simeq F_{K^+}(k^2) \simeq F_{B^+K^+J/\psi}(k^2), \\
F_{B^0}(k^2) &\simeq \frac{1}{3}-\frac{1}{3}\frac{m_\rho^2}{m_\rho^2-k^2} \\
&\simeq F_{K^0}(k^2) \simeq F_{B^0K^0J/\psi}(k^2), \\
F_{D^-}(k^2) &\simeq -\frac{2}{3}-\frac{1}{3}\frac{m_\rho^2}{m_\rho^2-k^2}, \\
F_{\bar{D^0}}(k^2) &\simeq -\frac{2}{3}+\frac{2}{3}\frac{m_\rho^2}{m_\rho^2-k^2}, \\
F_{D_S^+}(k^2) &\simeq 1,
\end{aligned}
\tag{19}
$$

where k is the momentum of photon and m_ρ is the mass of ρ meson. Then one can obtain the leading virtual-photon corrections to the ratios of the decay rates by replacing the photon propagator $1/k^2$ with the modified propagators as follows:

$$
\begin{aligned}
\int_{A_i,B_{1,2}} \frac{d^4k}{k^2} &\rightarrow \int_{A_i,B_{1,2}} d^4k \left(\frac{1}{k^2}-\frac{1}{k^2-m_\rho^2}+\frac{m_\rho^2}{3}\frac{\partial}{\partial m_\rho^2}\frac{1}{k^2-m_\rho^2}\right), \\
-\int_{B_3} \frac{d^4k}{k^2} &\rightarrow -\int_{B_3} d^4k \left(\frac{1}{k^2}-\frac{1}{k^2-m_\rho^2}\right), \\
-\int_{B_4} \frac{d^4k}{k^2} &\rightarrow -\int_{B_4} d^4k \left(\frac{1}{k^2}-\frac{1}{k^2-m_\rho^2}-\frac{m_\rho^2}{3}\frac{\partial}{\partial m_\rho^2}\frac{1}{k^2-m_\rho^2}\right),
\end{aligned}
\tag{20}
$$

where the subscripts A_i and B_j denote each loop shown in Fig. 3 and Fig. 4. Note that it is clear from the above equations that ultraviolet divergences arising from the one-loop calculation are naturally eliminated.

2.2 QED radiative corrections to decay rates

For actual calculation, it is convenient to introduce a small non-zero photon mass m_γ and obtain the analytic expressions of the virtual-photon corrections for the

point-like mesons first, so that the additional terms due to the ρ meson propagator in the **VMDM** can be simply obtained by replacing the photon mass with the ρ meson mass. Then, infrared divergences arising from the one-loop diagrams are expressed by $\ln m_\gamma$, and the linear terms of m_γ can be dropped whereas those of m_ρ cannot because the ρ meson is heavier than the K meson. Using the modified propagators given in Eq. (20), one can obtain the leading virtual-photon corrections to the ratios of the relevant decay rates as follows:

$$\delta^{+/0}_{virt}(J/\psi K) = \begin{cases} \dfrac{\alpha}{2\pi}\big(f_K(r_{J/\psi}, r_K; r_\gamma) + O(r_K)\big) & \text{(point-like mesons)}, \\ \dfrac{\alpha}{2\pi}\big(g_K(r_{J/\psi}, r_K, r_\rho; r_\gamma) + O(r_\rho)\big) & (\mathbf{VMDM}), \end{cases} \tag{21}$$

$$\delta^{+/0}_{virt}(D_S^+ D) = \begin{cases} \dfrac{\alpha}{2\pi} f_D(\sqrt{1-4r_D}; r_\gamma) & \text{(point-like mesons)}, \\ \dfrac{\alpha}{2\pi}\big(g_D(\sqrt{1-4r_D}, r_\rho; r_\gamma) + O(r_\rho)\big) & (\mathbf{VMDM}), \end{cases} \tag{22}$$

where

$$\begin{aligned} f_K(x,y;w) &= -4 + 2\big(2 - \ln(1-x)\big)\ln(1-x) - 2\mathrm{Li}_2(x) \\ &\quad - \left(1 - \frac{1}{2}\ln y\right)\ln y + \left(\ln\frac{(1-x)^2}{y} - 2\right)\ln w, \end{aligned} \tag{23}$$

$$\begin{aligned} g_K(x,y,v;w) &= -\frac{2}{3} + \frac{1}{3}\ln\frac{(1-x)^2}{y} + \frac{5\pi}{4}\sqrt{\frac{v}{y}}\left(1 - \frac{(3+x)\sqrt{y}}{1-x} + \frac{v}{5y}\right) \\ &\quad + \frac{v}{12y}\left[1 - \frac{3v}{y} - \left(10 - \frac{v}{y}\right)\ln\frac{v}{y}\right] \\ &\quad + \left(\ln\frac{(1-x)^2}{y} - 2\right)\ln\frac{w}{v}, \end{aligned} \tag{24}$$

$$
\begin{aligned}
f_D(x;w) &= \frac{1+x^2}{1-x^2}\ln\frac{4}{1-x^2}+\frac{\pi^2(1+x^2)}{3x}-\frac{2(2+x^2)}{x}\mathrm{Li}_2\left(\frac{1-x}{1+x}\right)\\
&\quad+\frac{2}{x}\mathrm{Li}_2\left(\left(\frac{1-x}{1+x}\right)^2\right)-\frac{2}{x}\ln\frac{1+x}{1-x}\ln\frac{2}{1+x}\\
&\quad+x\ln\frac{1+x}{1-x}\left(2\ln x-\frac{3-x^2}{1-x^2}-\frac{1}{2}\ln\frac{1+x}{1-x}-\ln w\right), \qquad (25)\\
g_D(x,v;w) &= -\frac{2}{3}+\frac{1}{3x}\ln\frac{1+x}{1-x}-\frac{\pi\sqrt{v}}{6x^2}\left[5\left(1-\frac{x^2}{2}\right)+\frac{7(1+2x^2)}{\sqrt{1-x^2}}\right]\\
&\quad+\frac{v}{3(1-x^2)}\left(17+4\ln\frac{4v}{1-x^2}\right)-x\ln\frac{1+x}{1-x}\ln\frac{w}{v}, \qquad (26)
\end{aligned}
$$

and where $r_P \equiv m_P^2/m_B^2$ and we use $m_{P^+} = m_{P^0} \equiv m_P$. In the above equations, $\ln r_K$ term in Eq. (23) has a mass singularity in the limit $m_K \to 0$ and it is removed by the same term in the real-photon corrections. In the **VMDM** there are additional terms such as m_ρ/m_K for non-zero m_ρ and m_K in general, and Eq. (24) was obtained for the K meson satisfying $m_\rho/2 < m_K < m_\rho$. In the limit $m_K \to 0$, the additional singular terms $\ln m_K$ and m_ρ/m_K in Eq. (24) produced by the ρ meson propagator are replaced by $\ln r_\rho$, and the function g_K can be rewritten as

$$
\begin{aligned}
g_K(x,y,v;w) &= -\frac{3}{4}+\frac{5\pi^2}{6}+2\left(\frac{1}{3}-\ln x\right)\ln(1-x)-2\mathrm{Li}_2(x)-2\mathrm{Li}_2(1-x)\\
&\quad-\left(1-\frac{1}{2}\ln y\right)\ln y+\left(\frac{8}{3}-2\ln(1-x)+\frac{1}{2}\ln v\right)\ln v\\
&\quad-\frac{5\pi(3+x)}{4(1-x)}\sqrt{v}+\left(\ln\frac{(1-x)^2}{y}-2\right)\ln w. \qquad (27)
\end{aligned}
$$

As for the D mesons, one can see the term m_ρ/m_D in Eq. (26) and this formula is valid for any other scalar meson P satisfying the condition $m_P > m_\rho$.

The real-photon corrections can be simply obtained by assuming that all mesons behave like point-like particles.

$$\delta^{+/0}_{real}(J/\psi K) = \frac{\alpha}{2\pi}\big(h_K(r_{J/\psi}, r_K; r_\gamma) + O(r_K)\big),$$
$$\delta^{+/0}_{real}(D_S^+ D) = \frac{\alpha}{2\pi} h_D(\sqrt{1-4r_D}; r_\gamma), \tag{28}$$

where

$$\begin{aligned} h_K(x,y;w) &= 9 - \frac{\pi^2}{3} - 4\sqrt{x} - \frac{2(1-3x)}{(1-x)^2} - 2\big(3 - \ln(1-x)\big)\ln(1-x) \\ &\quad - \frac{2x(1-4x+x^2)\ln x}{(1-x)^3} + \left(1 - \frac{1}{2}\ln y\right)\ln y \\ &\quad - \left(\ln\frac{(1-x)^2}{y} - 2\right)\ln w, \end{aligned} \tag{29}$$

$$\begin{aligned} h_D(x;w) &= 2x\left[\frac{\pi^2}{3} - \mathrm{Li}_2\left(\frac{1-x}{1+x}\right) - \mathrm{Li}_2\left(\left(\frac{1-x}{1+x}\right)^2\right)\right] \\ &\quad + x\ln\frac{1+x}{1-x}\left(1 + 2\ln x + 6\ln\frac{2}{1+x} + \frac{1}{2}\ln\frac{1+x}{1-x} + \ln w\right). \end{aligned} \tag{30}$$

Now one can obtain the total **QED** radiative corrections $\delta^{+/0}_{\mathbf{QED}} = \delta^{+/0}_{virt} + \delta^{+/0}_{real}$, and explicitly see that the infrared divergent terms expressed by $\ln r_\gamma$ in the virtual-photon corrections cancel out the same terms arising in the real-photon corrections in the usual way.

Using the standard values of the meson masses, we estimate the numerical values of the **QED** radiative corrections to the ratios of the decay rates:

$$\delta^{+/0}_{\mathbf{QED}}(J/\psi K) \simeq \begin{cases} -0.0012 & \text{(point-like mesons)}, \\ 0.0014 & (\mathbf{VMDM}), \end{cases} \tag{31}$$

$$\delta^{+/0}_{\mathbf{QED}}(D_S^+ D) \simeq \begin{cases} 0.0115 & \text{(point-like mesons)}, \\ -0.0013 & (\mathbf{VMDM}). \end{cases} \tag{32}$$

As a comparison, we list the radiative corrections for the point-like mesons too. In $B \to J/\psi K$ decays, the **QED** radiative correction to the ratio of the decay

rates is small because the real-photon correction is offset by the virtual-photon correction. On the other hand, the **QED** correction in $B \to D_S^+ D$ decays is sizable for the point-like mesons but significantly reduced in the **VMDM** due to the similar compensation between the real- and virtual-photon correction. In both cases, the deviations $\delta^{+/0}$ due to the isotopic mass splitting of the K and D mesons are about 0.0014, so that the total isospin violation effect in $B \to J/\psi K$ decays becomes about 0.3% in the **VMDM** while that in $B \to D_S^+ D$ decays becomes negligible. In different decay modes, of course, the corrections can be enhanced or reduced due to different final state masses.

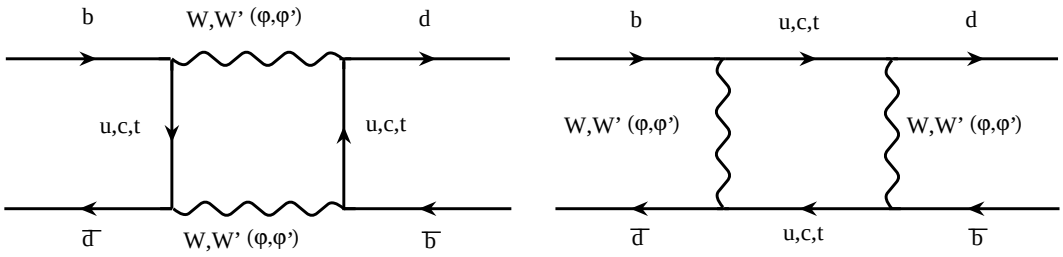

Figure 5: Box diagrams for $B^0\bar{B}^0$ mixing with the gauge bosons (W, W') and the unphysical scalar bosons (φ, φ').

3 $B\bar{B}$ mixing

3.1 Effective Hamiltonian for $B\bar{B}$ mixing

The effective Hamiltonian in the $B^0\bar{B}^0$ system is obtained by integrating out the internal loop in the box diagrams in Fig. 5 just as in the **SM**. We neglect external momenta and the d-quark mass, but the result is valid for general internal quark masses. One finds, using the Feynman-'t Hooft gauge, the charged gauge boson and the unphysical scalar boson contributions to $B^0\bar{B}^0$ mixing in a straightforward manner:

$$H_{eff}^{B\bar{B}} = H_{eff}^{SM} + H_{eff}^{RR} + H_{eff}^{LR} \tag{33}$$

with

$$\begin{aligned} H_{eff}^{SM} &= \frac{G_F^2 M_W^2}{4\pi^2} \sum_{i,j=u,c,t} \lambda_i^{LL} \lambda_j^{LL} \Bigg\{ \Bigg[\left(1 + \frac{x_i^2 x_j^2}{4}\right) f(x_i^2, x_j^2; 1) \\ &\quad -2 x_i^2 x_j^2 g(x_i^2, x_j^2; 1) \Bigg] (\bar{d}_L \gamma_\mu b_L)^2 + x_b^2 x_i^2 x_j^2 g(x_i^2, x_j^2; 1) (\bar{d}_L b_R)^2 \Bigg\}, \qquad (34) \\ H_{eff}^{RR} &= \frac{G_F^2 M_W^2}{4\pi^2} (\frac{g_R}{g_L})^2 \sum_{i,j=u,c,t} \lambda_i^{RR} \lambda_j^{RR} \zeta_g f(x_i^2 \zeta, x_j^2 \zeta; 1) (\bar{d}_R \gamma_\mu b_R)^2, \qquad (35) \end{aligned}$$

$$
\begin{aligned}
H_{eff}^{LR} &= \frac{G_F^2 M_W^2}{2\pi^2} \sum_{i,j=u,c,t} \Bigg\{ \lambda_i^{LR} \lambda_j^{RL} x_i x_j \zeta_g \big[4g(x_i^2, x_j^2; \zeta) \\
&\quad - f(x_i^2, x_j^2; \zeta) \big] (\bar{d}_L b_R)(\bar{d}_R b_L) + \ \lambda_i^{LL} \lambda_j^{LR} x_j x_b \xi_g^{+} \Bigg[x_i^2 \Big(g(x_i^2, x_j^2; 1) \\
&\quad - \frac{1}{4} f(x_i^2, x_j^2; 1) (\bar{d}_L \gamma_\mu b_L)^2 + \ (f(x_i^2, x_j^2; 1) - x_i^2 x_j^2 g(x_i^2, x_j^2; 1)) (\bar{d}_L b_R)^2 \Bigg] \\
&\quad + \lambda_i^{LL} \lambda_j^{RL} x_j x_b \xi_g^{-} \Bigg[x_i^2 \left(g(x_i^2, x_j^2; 1) - \frac{1}{4} f(x_i^2, x_j^2; 1) \right) (\bar{d}_L \gamma_\mu b_L)(\bar{d}_R \gamma_\mu b_R) \\
&\quad + (f(x_i^2, x_j^2; 1) - x_i^2 x_j^2 g(x_i^2, x_j^2; 1)) (\bar{d}_L b_R)(\bar{d}_R b_L) \Bigg] \Bigg\}, \qquad (36)
\end{aligned}
$$

where

$$
\frac{G_F}{\sqrt{2}} \equiv \frac{g_L^2}{8 M_W^2}, \quad \xi_g^{\pm} \equiv e^{\pm \alpha} \xi_g, \quad \lambda_i^{AB} \equiv V_{id}^{A*} V_{ib}^{B}, \quad x_i \equiv \frac{m_i}{M_W} \ (i = u, c, t), \qquad (37)
$$

and

$$
\begin{aligned}
f(x_i, x_j; \zeta) &= \frac{\ln(1/\zeta)}{(1-\zeta)(1-x_i\zeta)(1-x_j\zeta)} \\
&\quad + \left(\frac{x_i^2 \ln x_i}{(x_i - x_j)(1-x_i)(1-x_i\zeta)} + (i \longrightarrow j) \right), \\
g(x_i, x_j; \zeta) &= \frac{\zeta \ln(1/\zeta)}{(1-\zeta)(1-x_i\zeta)(1-x_j\zeta)} \\
&\quad + \left(\frac{x_i \ln x_i}{(x_i - x_j)(1-x_i)(1-x_i\zeta)} + (i \longrightarrow j) \right). \qquad (38)
\end{aligned}
$$

Although the form of the charged interactions in Eqs. (34)-(36) is independent of our particular choice of scalar representation, the Ward identities require that the box diagrams contributing to $B^0 \bar{B}^0$ mixing in the **LRM** are not gauge invariant [33]. In order to impose gauge invariance into our theory, we need to involve flavor-changing neutral Higgs bosons, but it is known that their contributions, even at the

tree-level as long as the mass of the flavor-changing Higgs boson is much heavier than $M_{W'}$,[4] are suppressed by approximately a factor of ζ compared to the above gauge boson contributions [34]. Therefore the above results, in the approximation of neglecting external momenta and the d-quark mass, provide the complete effective Hamiltonian contributing to $B^0\bar{B}^0$ mixing.

At this stage, in order to analyze the resulting effective Hamiltonian quantitatively, we need to consider specific forms of the right-handed quark mixing matrices V^R. If the model has manifest or pseudomanifest left-right symmetry, W_R mass has a stringent bound $M_{W_R} \geq 1.6$ TeV [24], and the W_R boson contributions to $B^0\bar{B}^0$ mixing and tree-level b decay are very small. But, in general, the form of V^R is not necessarily restricted to manifest or pseudomanifest symmetric types, so the W_R mass limit can be lowered to approximately 300 GeV by taking the following forms of V^R [35];

$$V_I^R = \begin{pmatrix} e^{i\omega} & \sim 0 & \sim 0 \\ \sim 0 & c_R e^{i\alpha_1} & s_R e^{i\alpha_2} \\ \sim 0 & -s_R e^{i\alpha_3} & c_R e^{i\alpha_4} \end{pmatrix}, \quad V_{II}^R = \begin{pmatrix} \sim 0 & e^{i\omega} & \sim 0 \\ c_R e^{i\alpha_1} & \sim 0 & s_R e^{i\alpha_2} \\ -s_R e^{i\alpha_3} & \sim 0 & c_R e^{i\alpha_4} \end{pmatrix}, \tag{39}$$

where c_R (s_R) $\equiv \cos\theta_R$ ($\sin\theta_R$) ($0^\circ \leq \theta_R \leq 90^\circ$). Here the matrix elements indicated as ~ 0 may be $\lesssim 10^{-2}$ and unitarity requires $\alpha_1 + \alpha_4 = \alpha_2 + \alpha_3$. From the $b \to c$ semileptonic decays of the B mesons, we can get an approximate bound $\xi_g \sin\theta_R \lesssim 0.013$ by assuming $|V_{cb}^L| \approx 0.04$ [36].

The effective Hamiltonians obtained in Eqs. (34)-(36) are then further simplified using the Glashow-Iliopoulos-Maiani (**GIM**) cancellation $\sum_{i=u,c,t} \lambda_i = 0$ and neglecting the u-quark mass:

[4]The tree-level flavor-changing neutral Higgs contributions with masses M_H of order $M_{W'}$ in the manifest or pseudomanifest left-right symmetric model were discussed in Ref. [25].

$$
\begin{aligned}
H_{eff}^{SM} &= \frac{G_F^2 M_W^2}{4\pi^2}(\lambda_t^{LL})^2 S(x_t^2)(\bar{d_L}\gamma_\mu b_L)^2, \qquad (40)\\
H_{eff}^{LR} &= \frac{G_F^2 M_W^2}{2\pi^2}\big\{[\lambda_c^{LR}\lambda_t^{RL}x_c x_t \zeta_g A_1(x_t^2,\zeta) \\
&\quad +\lambda_t^{LR}\lambda_t^{RL}x_t^2\zeta_g A_2(x_t^2,\zeta)](\bar{d_L}b_R)(\bar{d_R}b_L) \\
&\quad +\ \lambda_t^{LL}\lambda_t^{RL}x_b\xi_g^{-}[x_t^3 A_3(x_t^2)(\bar{d_L}\gamma_\mu b_L)(\bar{d_R}\gamma_\mu b_R) \\
&\quad +x_t A_4(x_t^2)(\bar{d_L}b_R)(\bar{d_R}b_L)]\big\}, \qquad (41)
\end{aligned}
$$

where

$$
\begin{aligned}
S(x) &= \frac{x(4-11x+x^2)}{4(1-x)^2} - \frac{3x^3\ln x}{2(1-x)^3},\\
A_1(x,\zeta) &= \frac{(4-x)\ln x}{(1-x)(1-x\zeta)} + \frac{(1-4\zeta)\ln\zeta}{(1-\zeta)(1-x\zeta)},\\
A_2(x,\zeta) &= \frac{4-x}{(1-x)(1-x\zeta)} + \frac{(4-2x+x^2(1-3\zeta))\ln x}{(1-x)^2(1-x\zeta)^2} \\
&\quad +\frac{(1-4\zeta)\ln\zeta}{(1-\zeta)(1-x\zeta)^2}, \qquad (42)\\
A_3(x) &= \frac{7-x}{4(1-x)^2} + \frac{(2+x)\ln x}{2(1-x)^3},\\
A_4(x) &= \frac{2x}{1-x} + \frac{x(1+x)\ln x}{(1-x)^2}.
\end{aligned}
$$

Note that $S(x)$ is the usual Inami-Lim function, $A_1(x,\zeta)$ is obtained by taking the limit $x_c^2 = 0$, and H_{eff}^{RR} is suppressed because it is proportional to ζ^2. Also, in the case of V_I^R, one can see that there is no significant contribution of H_{eff}^{LR} to $B^0\bar{B}^0$ mixing, so we concentrate on the second type V_{II}^R in this section. Moreover, if we consider **QCD** effect in $B\bar{B}$ mixing, the correction factors should be included in the functions S and A_i. However, there are many uncertainties such as hadronic matrix elements and new parameters in the **LRM** to prevent us from the precision

analysis at this stage, and the **QCD** corrections to $B\bar{B}$ mixing are not big enough to change our numerical estimate. Therefore we will ignore the **QCD** corrections to $B\bar{B}$ mixing for simplicity.

3.2 $B\bar{B}$ mixing matrix

The dispersive part of the $B^0\bar{B}^0$ mixing matrix element can be written as

$$M_{12} = M_{12}^{SM} + M_{12}^{LR} = M_{12}^{SM}\big\{1 + r_{LR}\big\}, \tag{43}$$

where

$$r_{LR} \equiv \frac{M_{12}^{LR}}{M_{12}^{SM}} = \frac{< \bar{B}^0|H_{eff}^{LR}|B^0 >}{< \bar{B}^0|H_{eff}^{SM}|B^0 >}. \tag{44}$$

For specific phenomenological estimates one needs the hadronic matrix elements of the operators in Eqs. (40), (41) in order to evaluate the mixing matrix element. We use the following parametrization:

$$\begin{aligned} < \bar{B}^0|(\bar{d}_L\gamma_\mu b_L)^2|B^0 > &= \frac{1}{3}B_1 f_B^2 m_B, \\ < \bar{B}^0|(\bar{d}_L\gamma_\mu b_L)(\bar{d}_R\gamma_\mu b_R)|B^0 > &= -\frac{5}{12}B_2 f_B^2 m_B, \\ < \bar{B}^0|(\bar{d}_L b_R)(\bar{d}_R b_L)|B^0 > &= \frac{7}{24}B_3 f_B^2 m_B, \end{aligned} \tag{45}$$

where

$$< 0|\bar{d}_\beta\gamma^\mu\gamma_5 b_\alpha|B^0 >= - < \bar{B}^0|\bar{d}_\beta\gamma^\mu\gamma_5 b_\alpha|0 >= -\frac{i f_B p_B^\mu}{\sqrt{2m_B}}\frac{\delta_{\alpha\beta}}{3}, \tag{46}$$

and where f_B is the B meson decay constant and B_i $(i = 1, 2, 3)$ are the bag factors. In the vacuum-insertion method [37], $B_i = 1$ in the limit $m_b \simeq m_B$. We will use $f_B B_i^{1/2} = (210 \pm 40)$ MeV for our numerical estimates [38]. In the case of V_I^R, there

is no significant contribution of H_{eff}^{LR} to $B^0\bar{B}^0$ mixing, so that $M_{12} = M_{12}^{SM}$ because $\lambda_t^{RL} \simeq 0$. In the case of V_{II}^R, using m_c=1.3 GeV, m_b=4.4 GeV, m_t=170 GeV, and $|V_{cd}^L| \approx 0.224$, and adopting the parametrization given in Eq. (45), one can express r_{LR} in terms of the mixing angle and phases in Eq. (39) as

$$\begin{aligned} r_{LR} \;\approx\; & l\Bigg\{17.3l\left(\frac{1-\zeta_g-(4.92-19.7\zeta_g)\ln(1/\zeta_g)}{1-5.47\zeta_g}\right)\zeta_g s_R^2 e^{i\delta_1} \\ & - 796\left(\frac{1-5.02\zeta_g-(0.498-1.99\zeta_g)\ln(1/\zeta_g)}{1-9.94\zeta_g+28.9\zeta_g^2}\right)\zeta_g s_R c_R e^{i\delta_2} \\ & - 8.93\xi_g s_R e^{i\delta_3}\Bigg\}, \end{aligned} \tag{47}$$

where $l = 0.008/|V_{td}^L|$, $\delta_1 = -2\beta + \alpha_2 - \alpha_3$, $\delta_2 = -\beta - \alpha_3 + \alpha_4$, $\delta_3 = -\beta - \alpha_3$, and the mixing phase $\alpha_\circ$ was absorbed in α_i by redefining $\alpha_i + \alpha_\circ \to \alpha_i$.

Now we investigate numerically the behavior of the ratio $|r_{LR}|$, which is the deviation of M_{12} from the **SM** value, under variation of $M_{W'}$, ξ_g, θ_R, and the phases in V^R, assuming $l = 1$. Although we use the average value of $|V_{td}|$, which might be different from the actual value of $|V_{td}^L|$, it should not affect the order of magnitude in our estimates. First, in order to see the dependence of $|r_{LR}|$ on the phases, we fix $M_{W'} = 800$ GeV, $\xi_g = 0.005$, $\theta_R = 15^\circ$, and set $\delta_3 = \pi$ because its effect is relatively much smaller than that of δ_1 and δ_2. The plot is shown in Fig. 6. From Eq. (47) and Fig. 6, one can see that $|r_{LR}|$ becomes maximal when $\delta_{1,3} = \pi$ and $\delta_2 = 0$, and minimal when $\delta_{1,2,3} = \pi$ if $\theta_R \lesssim 70^\circ$ (or $\delta_{1,2} = \pi$ and $\delta_3 = 0$ if $\theta_R \gtrsim 70^\circ$). This behavior also holds for other values of $M_{W'}$ and ξ_g. Since $|r_{LR}|$ is a continuously varying function of the phases, we can probe the allowed region for $|r_{LR}|$ with respect to the parameters $M_{W'}$, ξ_g, and θ_R. Next, we fix $M_{W'} = 800$ GeV, $\xi_g = 0.005$, and evaluate $|r_{LR}|$ by varying θ_R. Note that $|r_{LR}|$ can approach zero at a nonzero θ_R near 73° as shown in Fig. 7. Otherwise, it is larger than 1, which means

that generally it is possible to have $|M_{12}^{LR}| \gg |M_{12}^{SM}|$. In Fig. 8, we consider the behavior of $|r_{LR}|$ for $g_R/g_L \geq 0.5$, $\xi_g = 0.0004$, and $\theta_R = 14^\circ, 70^\circ$ as $M_{W'}$ is varied. The behavior of $|r_{LR}|$ exhibits a substantial dependence on $M_{W'}$, and $|r_{LR}|$ can be larger than 1 even for $M_{W'} \sim 2$ TeV. Moreover, it can be seen that $|r_{LR}|$ falls near $M_{W'} \sim 300$ GeV at certain angles and phases in the mixing matrices. This reflects the possibility of relatively light masses of W' compared to the previously known bound. We will return to this point in section 4. The dependence of $|r_{LR}|$ on ξ_g satisfying $\xi_g \sin\theta_R \lesssim 0.013$ at fixed $M_{W'} = 700$ GeV and $\theta_R = 14^\circ, 70^\circ$ is shown in Fig. 9. As one can see, $|r_{LR}|$ can be enhanced up to 10% of the **SM** contribution for the given inputs. Although its effect is smaller than that of other parameters, it is not negligible and can be dominant in $|r_{LR}|$ if the first two ζ dependent terms in Eq. (47) cancel each other.

As we mentioned previously, the average value of $|V_{td}|$ might be different from the actual value of $|V_{td}^L|$, and there is also ambiguity from errors in $f_B B_i^{1/2}$. Therefore the mass mixing ΔM_B^{SM} can be either much larger or smaller than ΔM_B^{exp}. However, if we assume that $0.5 \lesssim |\Delta M_B^{SM}/\Delta M_B^{expt}| \lesssim 2$, we can get specific bounds on the mass $M_{W'}$ and the angle θ_R using the experimental value $\Delta M_B^{exp} \simeq 0.472 \times 10^{12} s^{-1}$.

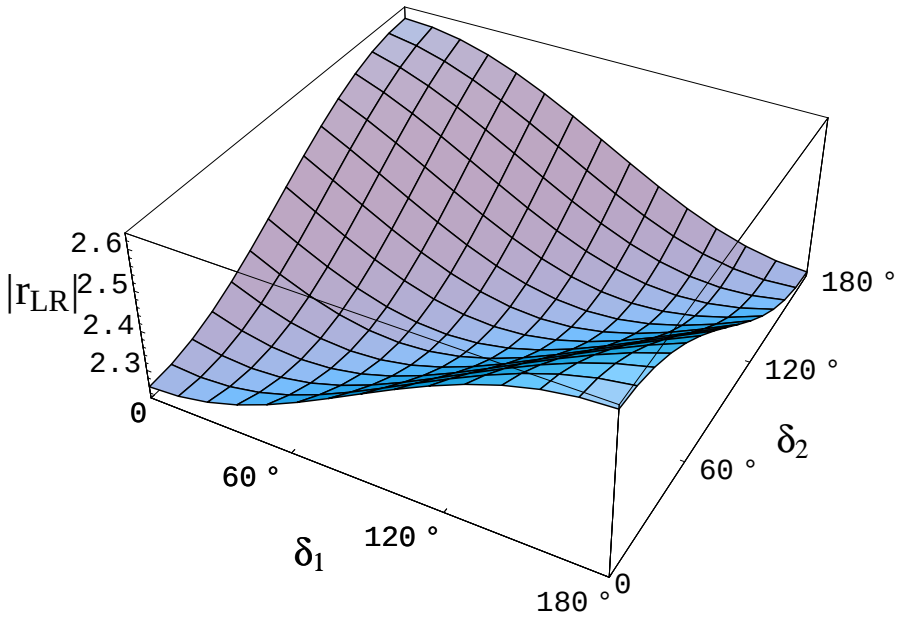

Figure 6: Behavior of the ratio $|r_{LR}|$ as $\delta_{1,2}$ are varied.

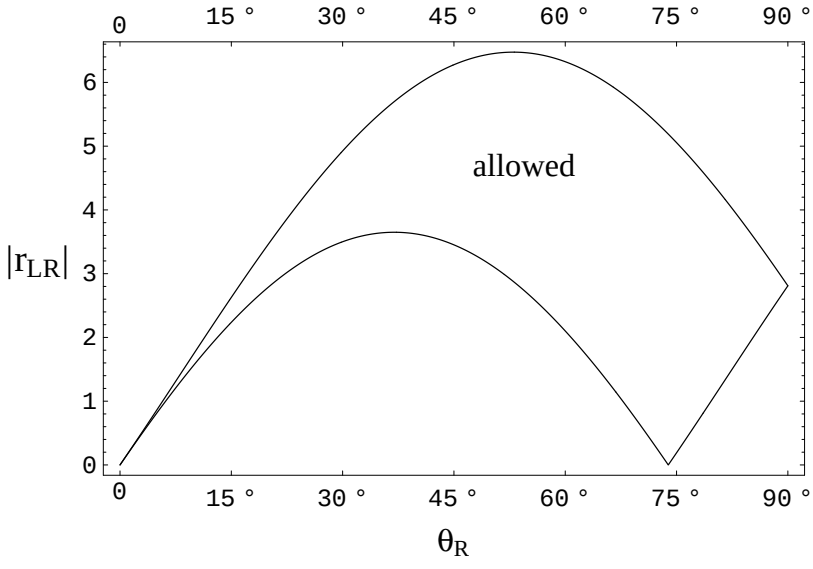

Figure 7: Allowed region for $|r_{LR}|$ and θ_R.

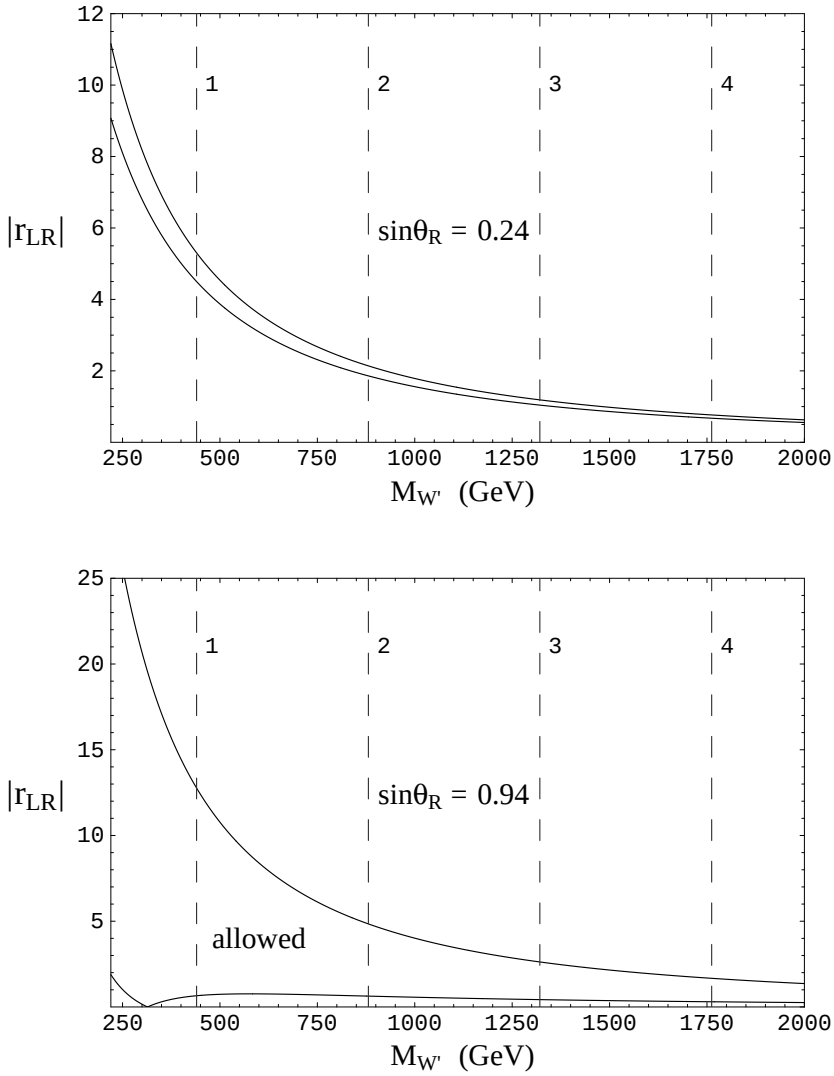

Figure 8: Allowed regions for $|r_{LR}|$ and $M_{W'}$ for $g_R/g_L \geq 0.5$. The dashed lines correspond to the lower bounds on $M_{W'}$ in Eq. (17) for the ratio g_R/g_L = 1,2,3, and 4, respectively.

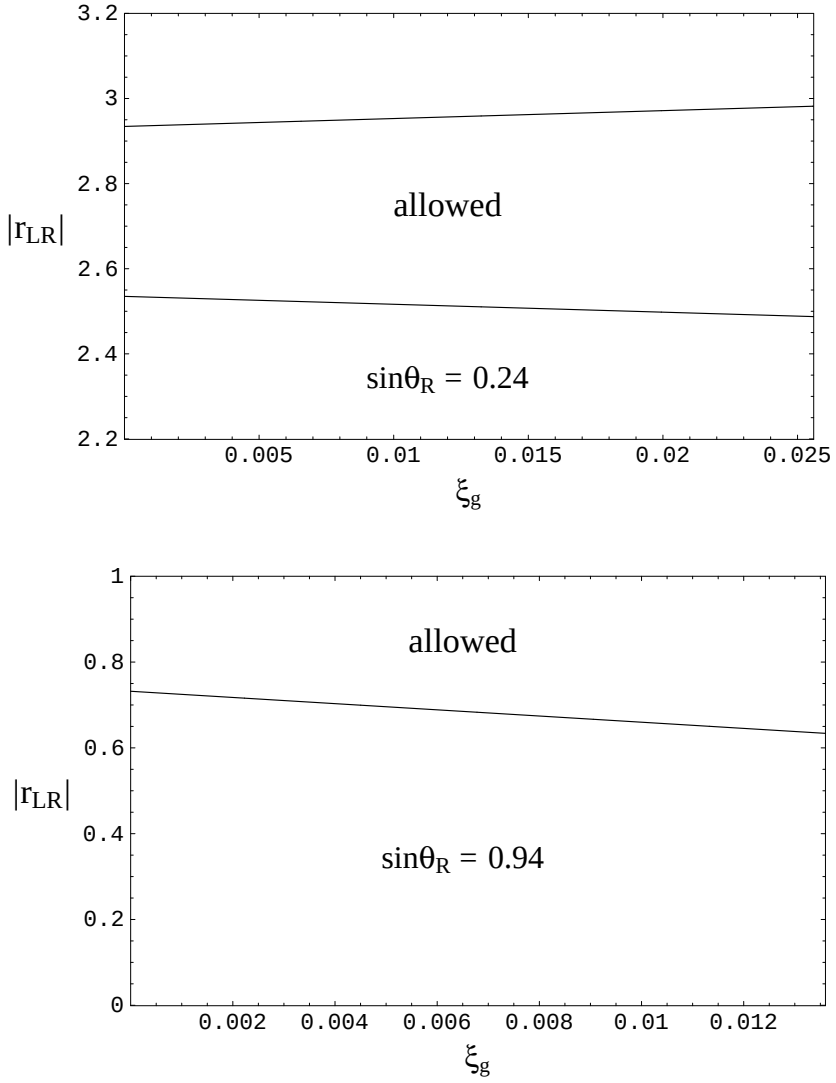

Figure 9: Allowed regions for $|r_{LR}|$ and ξ_g for $M_{W'} = 700$ GeV.

4 CP asymmetries in B decays

4.1 Effective Hamiltonian for $\Delta B = 1$ and $\Delta S = 1$ transition

The effective Hamiltonian approach is especially useful to describe the low-energy **QCD** effects of the full theory systematically. The low-energy effective Hamiltonian calculated within the framework of the operator product expansion (**OPE**) has a finite number of operators in a given order, which is dependent upon the structure of the model. In the **LRM**, the low energy effective Hamiltonian at the energy scale μ for $\Delta B = 1$ and $\Delta S = 1$ transition has the following form:

$$\begin{aligned}\mathcal{H}_{eff} &= \frac{G_F}{\sqrt{2}}\left[\sum_{\substack{i=1,2\\q=u,c}} \lambda_q^{LL} C_i^q O_i^q - \lambda_t^{LL}\left(\sum_{i=3}^{12} C_i O_i + C_7^\gamma O_7^\gamma + C_8^G O_8^G\right)\right] \\ &+ (C_i O_i \to C_i' O_i'), \end{aligned} \tag{48}$$

where

$$\begin{aligned} O_1^u &= (\bar{s}_\alpha u_\beta)_{\mathrm{V-A}} (\bar{u}_\beta b_\alpha)_{\mathrm{V-A}}\,, & O_2^u &= (\bar{s}_\alpha u_\alpha)_{\mathrm{V-A}} (\bar{u}_\beta b_\beta)_{\mathrm{V-A}}\,, \\ O_1^c &= (\bar{s}_\alpha c_\beta)_{\mathrm{V-A}} (\bar{c}_\beta b_\alpha)_{\mathrm{V-A}}\,, & O_2^c &= (\bar{s}_\alpha c_\alpha)_{\mathrm{V-A}} (\bar{c}_\beta b_\beta)_{\mathrm{V-A}}\,, \\ O_3 &= (\bar{s}_\alpha b_\alpha)_{\mathrm{V-A}} \sum_q (\bar{q}_\beta q_\beta)_{\mathrm{V-A}}\,, & O_4 &= (\bar{s}_\alpha b_\beta)_{\mathrm{V-A}} \sum_q (\bar{q}_\beta q_\alpha)_{\mathrm{V-A}}\,, \\ O_5 &= (\bar{s}_\alpha b_\alpha)_{\mathrm{V-A}} \sum_q (\bar{q}_\beta q_\beta)_{\mathrm{V+A}}\,, & O_6 &= (\bar{s}_\alpha b_\beta)_{\mathrm{V-A}} \sum_q (\bar{q}_\beta q_\alpha)_{\mathrm{V+A}}\,, \\ O_7 &= \frac{3}{2}(\bar{s}_\alpha b_\alpha)_{\mathrm{V-A}} \sum_q e_q (\bar{q}_\beta q_\beta)_{\mathrm{V+A}}\,, & O_8 &= \frac{3}{2}(\bar{s}_\alpha b_\beta)_{\mathrm{V-A}} \sum_q e_q (\bar{q}_\beta q_\alpha)_{\mathrm{V+A}}\,, \\ O_9 &= \frac{3}{2}(\bar{s}_\alpha b_\alpha)_{\mathrm{V-A}} \sum_q e_q (\bar{q}_\beta q_\beta)_{\mathrm{V-A}}\,, & O_{10} &= \frac{3}{2}(\bar{s}_\alpha b_\beta)_{\mathrm{V-A}} \sum_q e_q (\bar{q}_\beta q_\alpha)_{\mathrm{V-A}}\,, \end{aligned} \tag{49}$$

$$O_7^\gamma = \frac{e}{8\pi^2} m_b \bar{s}_\alpha \sigma^{\mu\nu}(1+\gamma_5) b_\alpha F_{\mu\nu}, \qquad O_8^G = \frac{g}{8\pi^2} m_b \bar{s}_\alpha \sigma^{\mu\nu}(1+\gamma_5) T^a_{\alpha\beta} b_\beta G^a_{\mu\nu},$$

$$O_{11}^u = \frac{m_b}{m_u} \left(\bar{s}_\alpha u_\beta\right)_{\mathrm{V-A}} \left(\bar{u}_\beta b_\alpha\right)_{\mathrm{V+A}}, \qquad O_{12}^u = \frac{m_b}{m_u} \left(\bar{s}_\alpha u_\alpha\right)_{\mathrm{V-A}} \left(\bar{u}_\beta b_\beta\right)_{\mathrm{V+A}},$$

$$O_{11}^c = \frac{m_b}{m_c} \left(\bar{s}_\alpha c_\beta\right)_{\mathrm{V-A}} \left(\bar{c}_\beta b_\alpha\right)_{\mathrm{V+A}}, \qquad O_{12}^c = \frac{m_b}{m_c} \left(\bar{s}_\alpha c_\alpha\right)_{\mathrm{V-A}} \left(\bar{c}_\beta b_\beta\right)_{\mathrm{V+A}},$$

and where α and β are color indices. $O_{1,2}$ are the standard current-current operators, $O_3 - O_6$ are the standard **QCD** penguin operators, $O_7 - O_{10}$ are the standard electroweak penguin operators, and O_7^γ and O_8^G are the standard photonic and gluonic magnetic operators, respectively [39]. Since we have additional $SU(2)_R$ group in the **LRM**, the operator basis is doubled by O_i' which are the chiral conjugates of O_i. Also new operators $O_{11,12}$ and $O'_{11,12}$ arise with mixed chiral structure of $O_{1,2}$ and $O'_{1,2}$ [27].

In order to calculate the Wilson coefficients $C_i(\mu)$, we first calculate them at $\mu = M_W$ scale. After performing a straightforward matching computation, we find the Wilson coefficients at W scale neglecting the u-quark mass:

$$\begin{aligned}
C_2^q(M_W) &= 1, \quad C_2^{q\prime}(M_W) = \zeta_g \lambda_q^{RR}/\lambda_q^{LL}, \\
C_7^\gamma(M_W) &= F(x_t^2) + A^{tb}\widetilde{F}(x_t^2), \\
C_7^{\gamma\prime}(M_W) &= A^{ts*}\widetilde{F}(x_t^2), \\
C_8^G(M_W) &= G(x_t^2) + A^{tb}\widetilde{G}(x_t^2), \\
C_8^{G\prime}(M_W) &= A^{ts*}\widetilde{G}(x_t^2),
\end{aligned} \tag{50}$$

where

$$
\begin{aligned}
F_0(x) &= \frac{x(7-5x-8x^2)}{24(x-1)^3} - \frac{x^2(2-3x)}{4(x-1)^4}\ln x, \\
\widetilde{F}_0(x) &= \frac{-20+31x-5x^2}{12(x-1)^2} + \frac{x(2-3x)}{2(x-1)^3}\ln x, \\
G_0(x) &= \frac{x(2+5x-x^2)}{8(x-1)^3} - \frac{3x^2}{4(x-1)^4}\ln x, \\
\widetilde{G}_0(x) &= -\frac{4+x+x^2}{4(x-1)^2} + \frac{3x}{2(x-1)^3}\ln x,
\end{aligned}
\tag{51}
$$

and

$$
A^{tD} = \xi_g \frac{m_t}{m_b}\frac{V_{tD}^R}{V_{tD}^L} e^{i\alpha_\circ} \ (D = b, s). \tag{52}
$$

All other coefficients vanish, and the terms proportional to ξ_g and ζ_g in the magnetic coefficients are neglected except the contribution coming from the virtual t-quark which gives m_t/m_b enhancement. Also the term proportional to ζ_g in the tree-level coefficient C_2' is not neglected because $\zeta_g \geq \xi_g$ and there is possible enhancement by the ratio of **CKM** angles $(\lambda_q^{RR}/\lambda_q^{LL})$ in the nonmanifest **LRM**.

The coefficients $C_i(\mu)$ at the scale $\mu = m_b$ can be obtained by evolving the coefficients $C_i(M_W)$ with the 28×28 anomalous dimension matrix applying the usual renormalization group procedure. Since the strong interaction preserves chirality, the 28×28 anomalous dimensional matrix decomposes into two identical 14×14 blocks. The **SM** 12×12 submatrix describing the mixing among $O_1 - O_{10}$, O_7^γ, and O_8^G can be found in Ref. [40], and the explicit form of the remaining 4×4 matrix describing the mixing among $O_{11,12}$, O_7^γ, and O_8^G, which partially overlaps with the **SM** 12×12 submatrix, can be found in Ref. [27]. The low energy Wilson coefficients at the scale $\mu = m_b$ in the **LL** approximation are then given by

$$
C_i(m_b) = \sum_{j,k} (S^{-1})_{ij} (\eta^{3\lambda_j/23}) S_{jk} C_k(M_W), \tag{53}
$$

where the λ_j's in the exponent of $\eta = \alpha_s(M_W)/\alpha_s(m_b)$ are the eigenvalues of the anomalous dimension matrix over $g^2/16\pi^2$ and the matrix S contains the corresponding eigenvectors. The result for the photonic and gluonic magnetic coefficients are calculated in Ref. [27] and in Ref. [26], respectively, and the rest of them related to our analysis can be found in Ref. [39].[5] Therefore we do not repeat them here, and lead the reader to the original papers. For 5 flavors, we have the following numerical values of $C_i(m_b)$ in **LL** precision using $\Lambda_{\overline{MS}}$=225 MeV, m_b=4.4 GeV, and m_t=170 GeV:

$$
\begin{aligned}
C_1^q = -0.308, \quad & C_1^{q\prime} = C_1^q \zeta_g \lambda_q^{RR}/\lambda_q^{LL}, \\
C_2^q = 1.144, \quad & C_2^{q\prime} = C_2^q \zeta_g \lambda_q^{RR}/\lambda_q^{LL}, \\
C_3 = 0.014, \quad C_4 = -0.030, \quad & C_5 = 0.009, \quad C_6 = -0.038, \\
C_7 = 0.045\alpha, \quad C_8 = 0.048\alpha, \quad & C_9 = -1.280\alpha, \quad C_{10} = 0.328\alpha, \\
C_7^\gamma = -0.317 - 0.546 A^{tb}, \quad & C_7^{\gamma\prime} = -0.546 A^{ts*}, \\
C_8^G = -0.150 - 0.241 A^{tb}, \quad & C_8^{G\prime} = -0.241 A^{ts*}.
\end{aligned}
\tag{54}
$$

Note that $C_3' - C_{10}'$ are negligible comparing to $C_7^{\gamma\prime}$ and $C_8^{G\prime}$ whereas $C_{1,2}'$ are not.[6] We will show that $C_{1,2}'$ are important to the absorptive parts in penguin-dominated B decays in the next subsection.

4.2 *CP* asymmetry in charged B meson decays

For charged B meson decays, the non-zero CP violating asymmetry defined as

[5] Although **QCD** correction factors in $C_{1,2}'$ are different from those in $C_{1,2}$ in general [41], we use an approximation $\alpha_s(M_{W'}) \simeq \alpha_s(M_W)$ for simplicity, which will not change our result.

[6] The numbers we obtained for $C_7^{\gamma(\prime)}$ and $C_8^{G(\prime)}$ are slightly different from those in Ref. [26] because they used m_t/m_b=60.

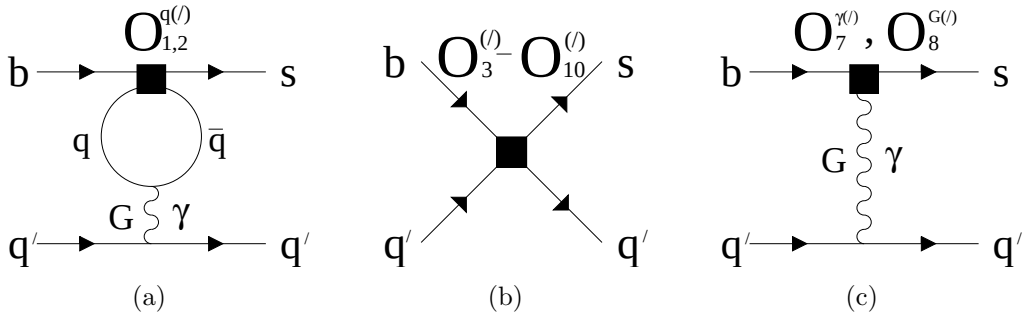

Figure 10: Diagrams for penguin-induced $b \to s\bar{q}'q'$ decays.

$$A_{CP} = \frac{\Gamma(B^+ \to f^+) - \Gamma(B^- \to f^-)}{\Gamma(B^+ \to f^+) + \Gamma(B^- \to f^-)} \tag{55}$$

originates from the superposition of CP-odd(violating) phases introduced by **CKM** matrix elements and CP-even(conserving) phases arising from the absorptive part of the amplitudes. Since we have obtained the relevant effective Hamiltonian in the previous subsection, it is quite straightforward to calculate the partial decay rates and CP asymmetries in $b \to s\bar{s}s$ decays. These decays are governed by three different types of penguin diagrams shown in Fig. 10. The absorptive part of the amplitudes arises at $O(\alpha_s)$ from the one-loop penguin diagrams with insertions of the operators $O_{1,2}^{(\prime)}$ shown in Fig. 10(a). The detailed calculation of the one-loop penguin matrix element of the operators $O_{1,2}$ in the **SM** is in Ref. [42] so that we can be very brief. The renormalized matrix elements of the operators $O_{1,2}^{(\prime)}$ in the **LL** approximation are given by

$$\begin{aligned} < O_1^{q(\prime)} >^{\rm peng} &= \frac{\alpha}{3\pi}\mathcal{I}(m_q, k, m_b) < P_\gamma^{(\prime)} >, \\ < O_2^{q(\prime)} >^{\rm peng} &= \frac{\alpha_s(m_b)}{8\pi}\mathcal{I}(m_q, k, m_b)\Big(< P_G^{(\prime)} > + \frac{8}{9}\frac{\alpha}{\alpha_s(m_b)} < P_\gamma^{(\prime)} > \Big), \end{aligned} \tag{56}$$

where

$$
\begin{aligned}
P_G^{(\prime)} &= O_4^{(\prime)} + O_6^{(\prime)} - \frac{1}{N_c}(O_3^{(\prime)} + O_5^{(\prime)}), \\
P_\gamma^{(\prime)} &= O_7^{(\prime)} + O_9^{(\prime)} \quad (N_c = 3),
\end{aligned} \tag{57}
$$

and

$$
\mathcal{I}(m, k, \mu) = 4\int_0^1 dx x(1-x) \ln\Big[\frac{m^2 - k^2 x(1-x)}{\mu^2}\Big], \tag{58}
$$

and where k is the momentum transferred by the gluon to the $(s, \bar{s})$ pair. As one can see from Eq. (58), different CP-even phases arise from the imaginary parts of the functions $\mathcal{I}(m_u, k, \mu)$ and $\mathcal{I}(m_c, k, \mu)$. On the other hand, the penguin operators $O_3 - O_{10}$ contribute to only the dispersive parts of the amplitudes and give tree-level penguin transition amplitudes shown in Fig. 10(b). Also, as shown in Fig. 10(c), we should include the tree-level diagram associated with the magnetic operators $O_7^{\gamma(\prime)}$ and $O_8^{G(\prime)}$ to the dispersive part of the amplitude. Using the factorization approximation [43], we use the following parametrization:

$$
\begin{aligned}
< O_7^{\gamma(\prime)} >^{\rm peng} &= -\frac{\alpha}{3\pi}\frac{m_b^2}{k^2} < P_\gamma^{(\prime)} >, \\
< O_8^{G(\prime)} >^{\rm peng} &= -\frac{\alpha_s}{4\pi}\frac{m_b^2}{k^2} < P_G^{(\prime)} > .
\end{aligned} \tag{59}
$$

Here k^2 is expected to be typically in the range $m_b^2/4 \le k^2 \le m_b^2/2$ [44]. We will use $k^2 = m_b^2/2$ for our numerical analysis.

Now we are ready to consider $B^\pm \to \phi K^\pm$ decays explicitly. Since the axial-vector parts of the operators do not contribute to the transition amplitudes in these decays we can simply use $< O_i >=< O_i' >$ with the help of the vacuum-insertion method [37]. Combining all operators, we obtain the following transition amplitude using the unitarity relation $\sum_{q=u,c,t} \lambda_q = 0$:

$$
\begin{aligned}
\mathcal{A}(B^- \to \phi K^-) &= \frac{G_F}{\sqrt{2}} \sum_{q=u,c} \lambda_q^{LL} \Bigg[\frac{\alpha_s(m_b)}{9\pi} \Big\{ C_2^q(m_b) \\
&\quad - \frac{7}{6} \frac{\alpha}{\alpha_s(m_b)} (3C_1^q(m_b) + C_2^q(m_b)) \Big\} \mathcal{I}(m_q, k, m_b) \\
&\quad - \frac{\alpha_s(m_b)}{9\pi} \Big\{ 4C_8^G(m_b) - 7 \frac{\alpha}{\alpha_s(m_b)} C_7^\gamma(m_b) \Big\} \\
&\quad + \frac{4}{3}(C_3(m_b) + C_4(m_b)) + C_5(m_b) + \frac{1}{3} C_6(m_b) \\
&\quad - \frac{1}{2} C_7(m_b) - \frac{1}{6} C_8(m_b) - \frac{2}{3}(C_9(m_b) + C_{10}(m_b)) \Bigg] \\
&\quad \times X^{(B^- K^-, \phi)} + (C_i \to C_i'),
\end{aligned} \tag{60}
$$

where $X^{(B^- K^-, \phi)} \equiv < \phi | \bar{s} \gamma_\mu s | 0 > < K^- | \bar{s} \gamma^\mu b | B^- >$. The amplitude $\mathcal{A}(B^+ \to \phi K^+)$ is simply obtained from $\mathcal{A}(B^- \to \phi K^-)$ by replacing $\lambda_q^{LL} \to \lambda_q^{LL*}$ and $C_i^{(\prime)} \to C_i^{(\prime)*}$. In the **SM**, nonzero *CP* asymmetry arises from the superposition of the *CP*-odd phase γ in V_{ub}^L and the different *CP*-even phases arising from the function $\mathcal{I}(m_q, k, m_b)$ due to the mass difference between c- and u-quark. The resulting *CP* asymmetry is known to be very small $\sim O(10^{-2})$ [42, 45] because the magnitude of the absorptive part is much smaller than that of the dispersive part. Using the numbers in Eq. (54), m_c=1.3 GeV, and $\mathrm{Arg}[V_{ub}^L] = -59^\circ$, we can estimate the **SM** value of *CP* asymmetry:

$$
A_{CP}^{SM}(B^\pm \to \phi K^\pm) \simeq 7.3 \times 10^{-3}. \tag{61}
$$

As stated earlier, if the model has manifest left-right symmetry, the W_R mass has a stringent bound $M_{W_R} \geq$1.6 TeV, and its contribution to the decay amplitude is very small so that *CP* asymmetry in the manifest **LRM** should be very small as well. Since this value is small and our purpose is to estimate the possible large

right-handed current contribution, we take a limit $\mathcal{I}(m_c,k,\mu)=\mathcal{I}(m_u,k,\mu)$ in order to get around the uncertainty of V_{ub}^L obtained under the **SM** framework and clearly see the right-handed current contribution. Then we can express $\mathcal{A}(B^-\to\phi K^-)$ in terms of new parameters ζ_g, ξ_g, and θ_R for two types of V^R in Eq. (39) in the **LRM** using the unitarity relation $\sum_{q=u,c,t}\lambda_q=0$ and the numbers in Eq. (54) again as follows:

$$\begin{aligned}
\mathcal{A}(B^-\to\phi K^-)_I &\simeq -\frac{G_F}{\sqrt{2}}\Big\{-2.87e^{i\varphi_1}+23.1e^{i\varphi_2}\zeta_g c_R s_R e^{i(\alpha_4-\alpha_3)} \\
&\quad +10.1\xi_g(c_R e^{i\alpha_4}-25 s_R e^{i\alpha_3})\Big\}\times 10^{-3}X^{(B^-K^-,\phi)}, \\
\mathcal{A}(B^-\to\phi K^-)_{II} &\simeq -\frac{G_F}{\sqrt{2}}\Big\{-2.87e^{i\varphi_1}+10.1\xi_g c_R e^{i\alpha_4}\Big\}\times 10^{-3}X^{(B^-K^-,\phi)}, \quad (62)
\end{aligned}$$

where $(\varphi_1,\varphi_2)=(-14.9^\circ,-53.1^\circ)$ are CP-even phases. One can clearly see here that the ζ_g term coming from the coefficients $C'_{1,2}$ is not negligible in case of V_I^R. Likewise, the transition amplitude in $B^-\to\phi K^{*-}$ decays can be easily obtained by using $<O_i>=-<O_i'>$ because K^{*-} is a vector particle:

$$\begin{aligned}
\mathcal{A}(B^-\to\phi K^{*-})_I &\simeq -\frac{G_F}{\sqrt{2}}\Big\{2.87e^{i\varphi_1}+23.1e^{i\varphi_2}\zeta_g c_R s_R e^{i(\alpha_4-\alpha_3)} \\
&\quad +10.1\xi_g(-c_R e^{i\alpha_4}-25 s_R e^{i\alpha_3})\Big\}\times 10^{-3}X^{(B^-K^{*-},\phi)}, \\
\mathcal{A}(B^-\to\phi K^{*-})_{II} &\simeq -\frac{G_F}{\sqrt{2}}\Big\{2.87e^{i\varphi_1}-10.1\xi_g c_R e^{i\alpha_4}\Big\}\times 10^{-3}X^{(B^-K^{*-},\phi)}, \quad (63)
\end{aligned}$$

where $X^{(B^-K^{*-},\phi)}\equiv<\phi|\bar{s}\gamma_\mu s|0><K^{*-}|\bar{s}\gamma^\mu\gamma_5 b|B^->$. Although the CP asymmetry in $B^-\to\phi K^-$ decays should be the same as that in $B^-\to\phi K^{*-}$ decays in the **SM**, they can be different in **LRM** so that the measured difference of CP asymmetries between them may give the size of the **NP** effects.

The current data on the CP asymmetries in $B^-\to\phi K^-$ and $B^-\to\phi K^{*-}$ decays are [46]

$$A_{CP}^{\rm expt}(B^\pm \to \phi K^\pm) = 0.05 \pm 0.20 \pm 0.03,$$

$$A_{CP}^{\rm expt}(B^\pm \to \phi K^{*\pm}) = 0.43 \,^{+\,0.36}_{-\,0.30} \pm 0.06. \quad (64)$$

The **SM** value in Eq. (61) lies in the range of $A_{CP}^{\rm expt}(B^\pm \to \phi K^\pm)$, but a little off the range of $A_{CP}^{\rm expt}(B^\pm \to \phi K^{*\pm})$. In order to explicitly compare these values with the theoretical estimates in the **LRM**, we first plot $A_{CP}(B^\pm \to \phi K^\pm)$ and $A_{CP}(B^\pm \to \phi K^{*\pm})$ in the case of V_I^R in Fig. 11 for the typical values ζ_g=0.01, ξ_g=0.008, and $\theta_R = 70^\circ$ as $\alpha_{3,4}$ are varied. In the figure, *CP* asymmetry is drastically changing by varying α_3, and this behavior holds for other values of ζ_g, ξ_g, and θ_R. For the given inputs, $A_{CP}(B^\pm \to \phi K^\pm)$ and $A_{CP}(B^\pm \to \phi K^{*\pm})$ can be different by about 0.5. In the case of V_{II}^R, one can see from Eqs. (62), (63) that $A_{CP}(B^\pm \to \phi K^\pm)$ $= A_{CP}(B^\pm \to \phi K^{*\pm})$ because it has no dependance of ζ_g and α_3 unlike the previous case. In Fig. 12, we fix ξ_g=0.01, and evaluate *CP* asymmetry by varying θ_R and α_4. It shows that *CP* asymmetry is very small with a small parameter ξ_g. Therefore, if we observe large *CP* asymmetry or any difference between $A_{CP}(B^\pm \to \phi K^\pm)$ and $A_{CP}(B^\pm \to \phi K^{*\pm})$, the second type of mass mixing matrix V_{II}^R is disfavored.

4.3 *CP* asymmetry in neutral B meson decays

In the case of the neutral B meson decays into *CP* self-conjugate final states f, mixing induced *CP* asymmetry can be expressed by the parametrization invariant quantity λ defined by [9]

$$\lambda \equiv \eta_f \left(\frac{q}{p}\right)_B \frac{\mathcal{A}(\bar{B}^0 \to \bar{f})}{\mathcal{A}(B^0 \to f)}, \qquad \left(\frac{q}{p}\right)_B \simeq \frac{M_{12}^*}{|M_{12}|}\ , \quad (65)$$

where η_f=1(-1) for a *CP*-even(odd) final state f and M_{12} is the dispersive part of the $B^0\bar{B}^0$ mixing matrix element defined in Eq. (43). The *CP* angle β mentioned

earlier is simply the imaginary part of λ in $B \to J/\psi K_S$ decays in the **SM**:

$$\sin 2\beta = \mathrm{Im}\lambda(B \to J/\psi K_S) \simeq \mathrm{Im}\lambda(B \to \phi K_S). \tag{66}$$

In the general **LRM**, the two types of V^R give us two distinct results. Since $B \to J/\psi K_S$ decay is governed by the tree-level amplitude, the transition amplitude is given by

$$\begin{aligned}
\mathcal{A}(B \to J/\psi K_s)_I &\simeq \frac{G_F}{\sqrt{2}}\lambda_c^{LL}\Big\{1 + 25(c_R s_R \zeta_g e^{-i(\alpha_2-\alpha_1)} \\
&\quad -2 s_R \xi_g e^{-i\alpha_2})\Big\} X^{(BK_s,J/\psi)}, \\
\mathcal{A}(B \to J/\psi K_s)_{II} &\simeq \frac{G_F}{\sqrt{2}}\lambda_c^{LL}\Big\{1 - 50 s_R \xi_g e^{-i\alpha_2}\Big\} X^{(BK_s,J/\psi)},
\end{aligned} \tag{67}$$

where $X^{(BK_s,J/\psi)} \equiv < J/\psi|\bar{c}\gamma_\mu c|0 >< K_s|\bar{s}\gamma^\mu b|B^\circ >$, and we ignored the $K\bar{K}$ mixing. The transition amplitude in $B \to \phi K_S$ decays can be simply obtained from Eq. (62) by replacing the hadronic matrix element $X^{(B^-K^-,\phi)} \to X^{(BK_s,\phi)}$.

For illustration of the possible effect of the new interaction on the mixing induced CP asymmetry, we assume that $\beta = 20^\circ$ and $l = 1$, and show that the region of parameters α_i where $\mathrm{Im}\lambda(B \to J/\psi K_S) \simeq 0.73$ and $\mathrm{Im}\lambda(B \to \phi K_S) \simeq -0.39$ since $|\lambda| \approx 1$. To do so, we need to find an appropriate set of parameters ζ_g, ξ_g, and θ_R yielding a large difference $\Delta_{CP} \equiv \mathrm{Im}\lambda(B \to J/\psi K_S) - \mathrm{Im}\lambda(B \to \phi K_S)$. First, we evaluate Δ_{CP} in the case of V_I^R for $\zeta_g = \xi_g = 0.01$, $\alpha_{1,2} = 0$ by varying θ_R and α_3 in Fig. 13(a). In the figure, Δ_{CP} becomes maximal near $\alpha_3 \sim -120^\circ$ and increases as θ_R increases, and this behavior holds for other values of fixed parameters. Since we assumed that Δ_{CP} is larger than 1, we fix $\alpha_3 = -120^\circ$, and evaluate Δ_{CP} in Fig. 13(b) for $\alpha_{1,2} = 0$ and $\xi_g = \zeta_g$ by varying θ_R and ζ_g. One can see from the figure that Δ_{CP} approaches 1 for $\zeta_g \gtrsim 0.01$ and $\theta_R \gtrsim 10^\circ$, and its variation is small.

After repeating this analysis, we get a probable set of parameter values $\zeta_g = 0.01$, $\xi_g = 0.008$, $\theta_R = 70°$, and $\alpha_3 = -120°$. Using these values, we plot the contours corresponding to $\mathrm{Im}\lambda(B \to J/\psi K_S) = 0.73$ and $\mathrm{Im}\lambda(B \to \phi K_S) = -0.39$ in the parameter space of $\alpha_{1,2}$ in Fig. 14. We may conclude, as a result of the obtained figures, that the manifest or pseudomanifest **LRM** is disfavored under the given assumptions. In a similar way to the case of V_I^R, the results of the analysis of the mixing induced CP asymmetries in the case of V_{II}^R are represented in Fig. 15 and Fig. 16.

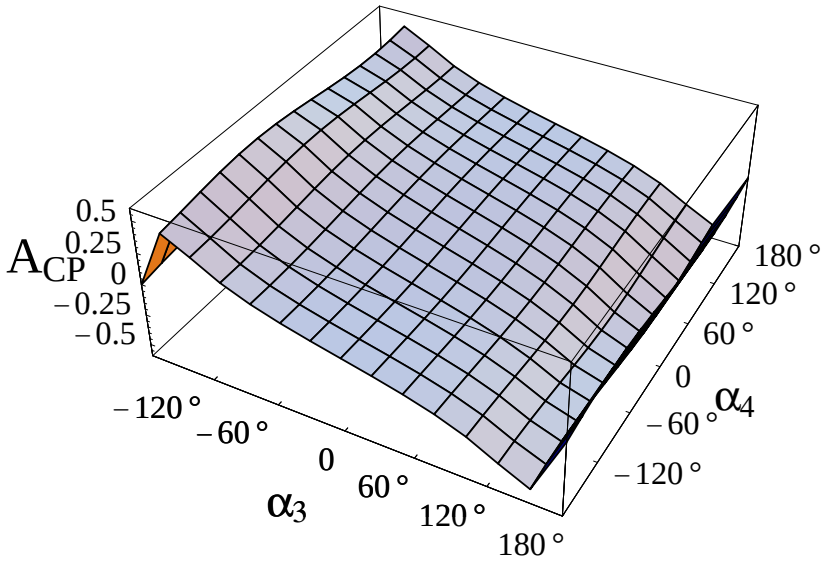

(a) $B^{\pm} \to \phi K^{\pm}$ decays

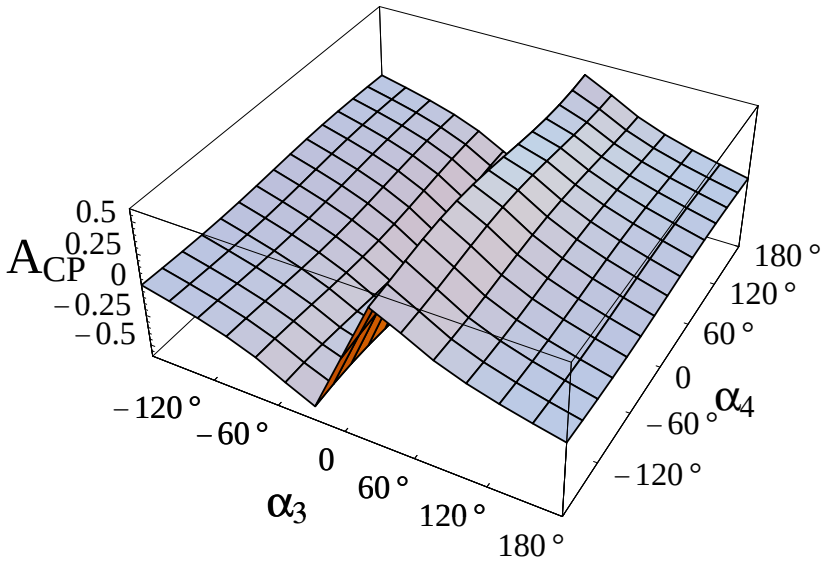

(b) $B^{\pm} \to \phi K^{*\pm}$ decays

Figure 11: Behavior of A_{CP} as $\alpha_{3,4}$ are varied in the case of V_I^R.

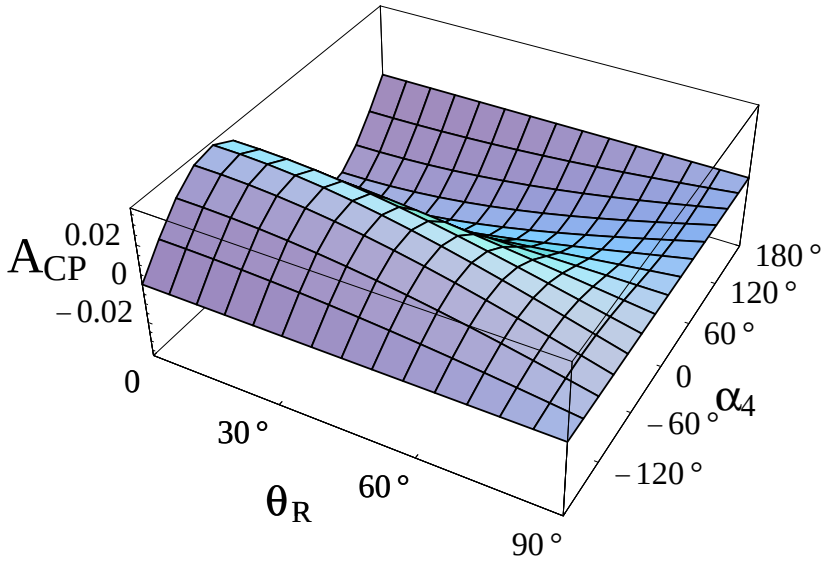

Figure 12: Behavior of $A_{CP}(B^{\pm} \to \phi K^{(*)\pm})$ as θ_R and α_4 are varied in the case of V_{II}^R.

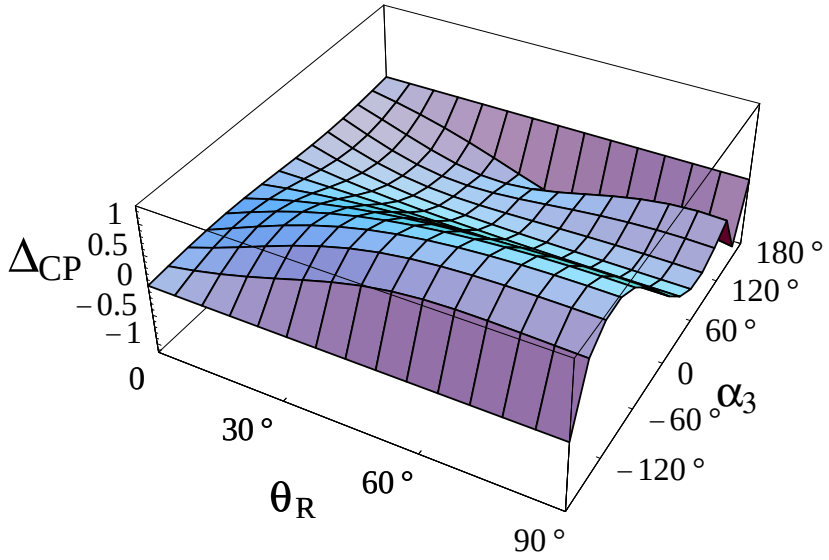

(a)

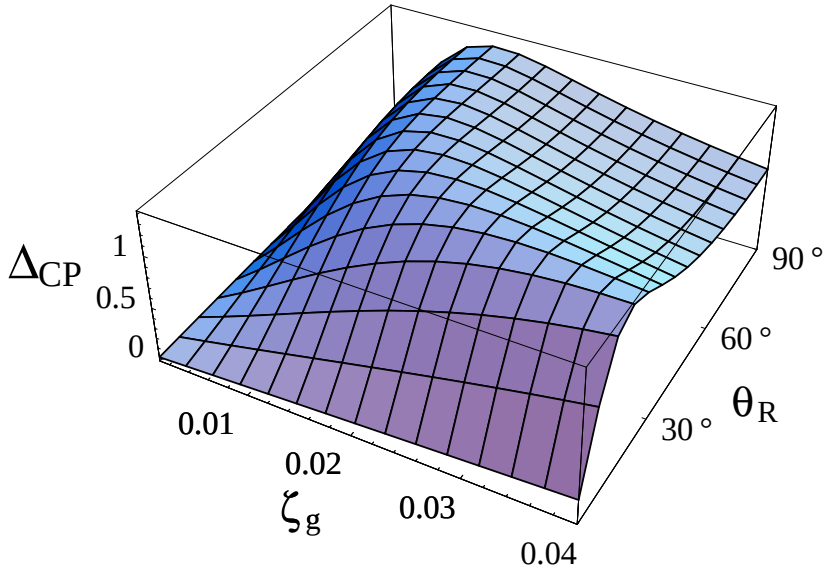

(b)

Figure 13: Behavior of the CP asymmetry difference Δ_{CP} between $B \to J/\psi K_S$ and $B \to \phi K_S$ decays in the case of V_I^R.

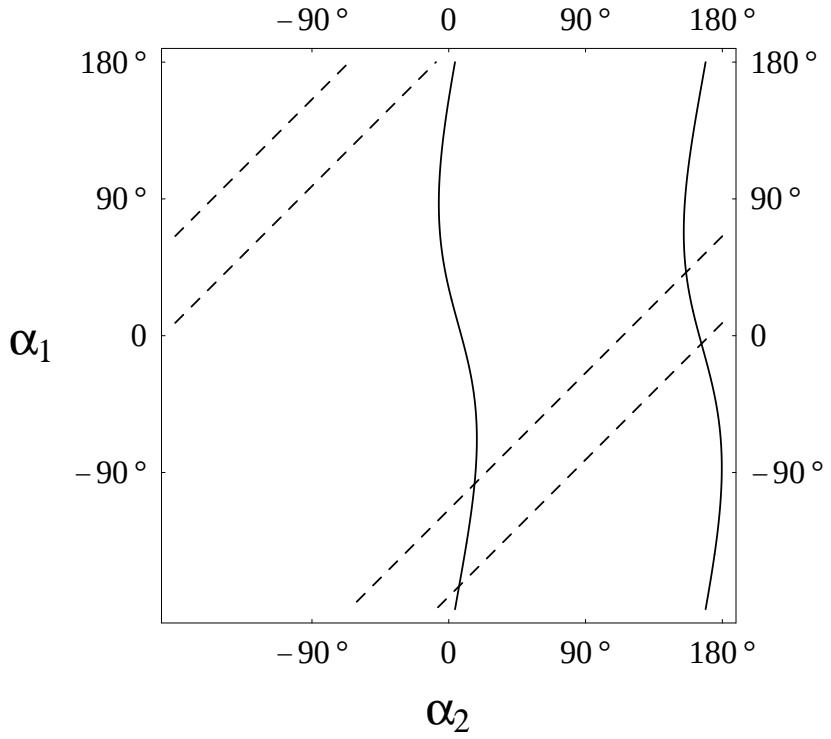

Figure 14: Contour plot corresponding to $\mathrm{Im}\lambda(B \to J/\psi K_S) = 0.73$ (solid line) and $\mathrm{Im}\lambda(B \to \phi K_S) = -0.39$ (dashed line) for $\sin 2\beta = 0.64$ in the case of V_I^R.

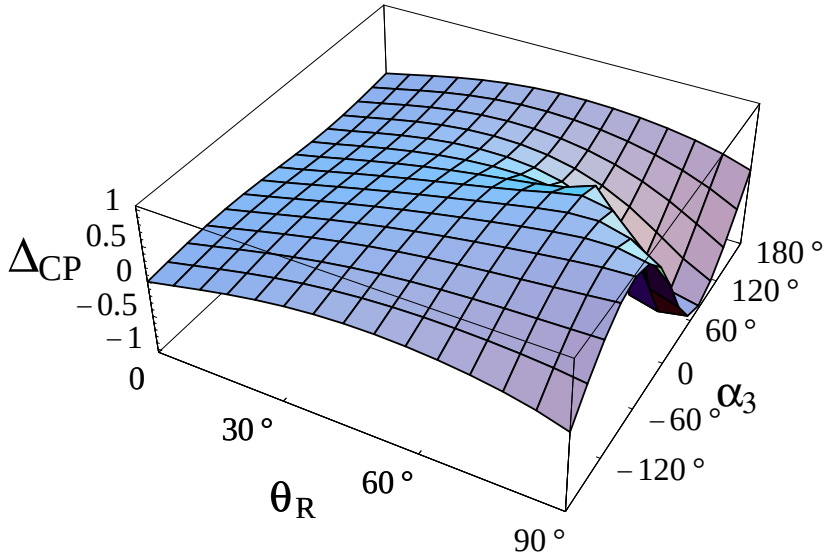

(a)

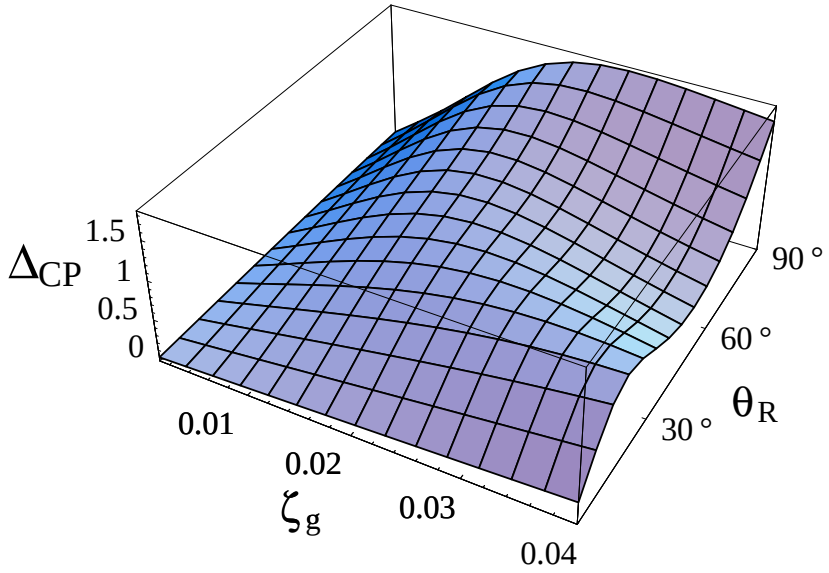

(b)

Figure 15: Behavior of the CP asymmetry difference Δ_{CP} between $B \to J/\psi K_S$ and $B \to \phi K_S$ decays in the case of V_{II}^R.

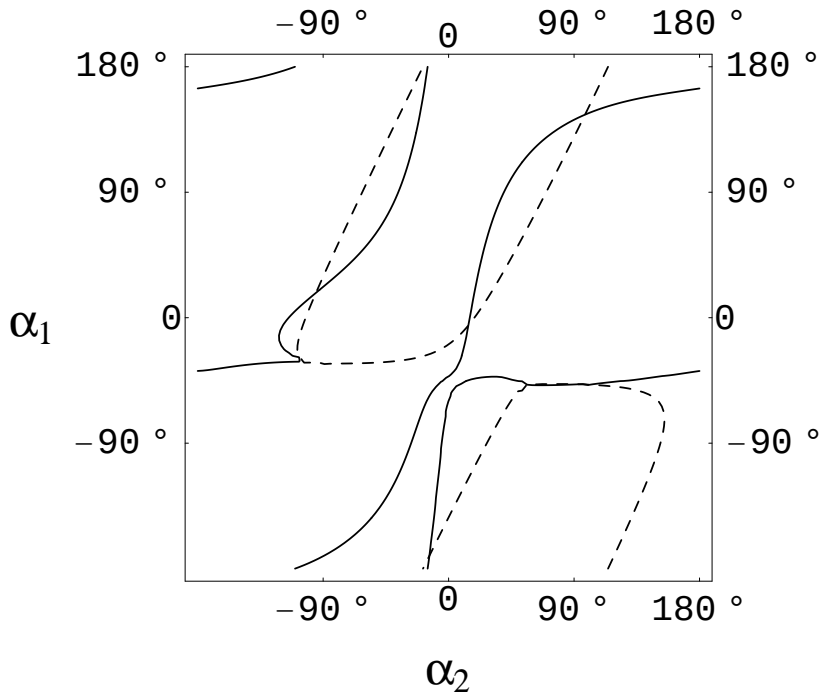

Figure 16: Contour plot corresponding to $\mathrm{Im}\lambda(B \to J/\psi K_S) = 0.73$ (solid line) and $\mathrm{Im}\lambda(B \to \phi K_S) = -0.39$ (dashed line) for $\sin 2\beta = 0.64$ in the case of V_{II}^R.

5 Summary

In summary, we studied three major aspects in the B meson system in the **SM** and the **LRM**: **QED** radiative corrections, $B\bar{B}$ mixing, and CP asymmetry. At present B-factory experiments, a measurement of the B^+B^- to $B^0\bar{B}^0$ production ratio $R^{+/0}$ in e^+e^- annihilation is essential for observing large CP violating effects and accurate determination of the **SM** parameters such as quark-mixing matrix elements. The practical measurements of the ratio $R^{+/0}$ use the ratio of some isospin-related decay rates where the isospin-violating effect due to mass differences between those decays is very small. In decays of these types, however, there is still an isospin violation due to **QED** radiative corrections which may affect the measurements of $R^{+/0}$. Due to this reason, we explicitly calculated the **QED** corrections to the ratios of the two different types of B decays, $B^+ \to J/\psi K^+$ and $B^0 \to J/\psi K^0$ (VP type) decays as well as $B^+ \to D_S^+ \bar{D}^0$ and $B^0 \to D_S^+ D^-$ (PP type) decays. The estimated **QED** corrections to the ratios of those decay rates range approximately from 0.1% to 1% depending on the structures of the final state mesons. Therefore, in order to obtain the production ratio $R^{+/0}$ more accurately in precision measurements, one should include the **QED** correction or find an appropriate decay mode where the isotopic violation due to the **QED** effects is very small. As well as the determination of $R^{+/0}$, the obtained results are also of importance in the study of the structure of hadron. We explicitly show in Eq. (31) and Eq. (32) how the form factors of the mesons affect the radiative corrections. This work can be used to test the model itself and will be useful for the study of the form factors when future experiments are available to access the ratios of the decay rates.

The decay $B^0 \to J/\psi K^0$ is a transition into a CP eigenstate with eigenvalue

-1, and originates from the $b \to \bar{c}c\bar{s}$ tree-level transition. It is especially important as a benchmark mode since large CP-violating effects were observed recently. In the **SM**, CP violation in the above decay mode is expressed by a phase β in the **CKM** matrix through $B^0\bar{B}^0$ mixing, but the present experimental results revealing large CP violation are not simply explained with this single phase. Therefore we reexamined $B^0\bar{B}^0$ mixing and CP asymmetry in B decays in the **LRM** since it is one of the simplest extensions of the **SM** gauge group and a complement of the purely left-handed nature of the **SM**. In the **LRM**, if one does not impose manifest or pseudomanifest left-right symmetry, the W' contributions to $B^0\bar{B}^0$ mixing and CP asymmetry in B^0 decays are highly dependent upon the phases in the mass mixing matrix $V^{L,R}$. For certain phases, the contribution of W' with a heavy mass about a few TeV to $B^0\bar{B}^0$ mixing can be sizeable. On the other hand, there is also the possibility of the existence of W' with a light mass about a few hundred GeV, whose contribution can be either very large or small, and so the contribution of the mixing angle ξ is not negligible. Since the existence of a light W' requires a small g_R, $g_R \lesssim g_L$, one can see from Eq. (43) and Fig. 8 that its contribution is limited. Therefore even assuming that $\Delta M_B^{LR} \lesssim \Delta M_B^{SM}$, we find that there is a possibility of a light W' with a mass $M_{W'} \sim 300$ GeV.

In addition to $B^0 \to J/\psi K^0$ decays, the CP angle β can be measured in $B^0 \to \phi K_S$ decays which originate from the $b \to s\bar{s}s$ penguin-induced transition. In the **SM**, CP asymmetry in $B^0 \to J/\psi K^0$ decays should be very close to that in $B^0 \to \phi K_S$ decays, but the present experiments show a large discrepancy between them. Based on these preliminary experimental results, we explicitly evaluated the sizes of the **NP** contributions to CP asymmetry in those decays using the effective Hamiltonian approach. We find that the manifest or pseudomanifest **LRM** is disfa-

vored, and the bounds of the new parameters are restricted as shown in Figs. 13-16. Similar argument can be made in charged B meson decays such as $B^{\pm} \to \phi K^{(*)\pm}$ decays where the **SM** contribution to CP asymmetry is very small. In the **LRM**, V_I^R is more probable than V_{II}^R if CP asymmetries in those decays are large or different from each other. Furthermore, one can see from Fig. 11 and Fig. 12 that the contribution of the obtained parameter sets from Fig. 14 and Fig. 16 under the given assumption reduces the size of CP asymmetries in $B^{\pm} \to \phi K^{(*)\pm}$ decays. In this way, CP asymmetries in other mixing induced decays such as $B \to \phi K^*$ can be estimated systematically, and all of these analysis of possible **NP** contributions can be tested once the experimental results are confirmed.

References

[1] CLEO Collaboration, J.P. Alexander *et al.*, Phys. Rev. Lett. **86**, 2737 (2001); S.B. Athar *et al.*, Phys. Rev. D **66**, 052003 (2002).

[2] BABAR Collaboration, B. Aubert *et al.*, Phys. Rev. D **65**, 032001 (2002); *ibid.* **69**, 071101 (2004).

[3] Belle Collaboration, N.C. Hastings *et al.*, Phys. Rev. D **67**, 052004 (2003).

[4] BABAR Collaboration, B. Aubert *et al.*, hep-ex/0504001 .

[5] D. Atwood and W.J. Marciano, Phys. Rev. D **41**, 1736 (1990).

[6] G.P. Lepage, Phys. Rev. D **42**, 3251 (1990); N. Byers and E. Eichten, Phys. Rev. D **42**, 3885 (1990); R. Kaiser, A.V. Manohar, and T. Mehen, Phys. Rev. Lett. **90**, 142001 (2003).

[7] M.B. Voloshin, Mod. Phys. Lett. A **18**, 1783 (2003); hep-ph/0402171 .

[8] M.B. Voloshin, Phys. Lett. B **433**, 419 (1998).

[9] For a recent review, see I.I. Bigi and A.I. Sanda, *CP Violation* (Cambridge University Press, Cambridge, England, 2000).

[10] Y. Nir, Nucl. Phys. B (Proc. Suppl.) **117**, 111 (2003) .

[11] L. Wolfenstein, Phys. Rev. Lett. **51**, 1945 (1983).

[12] Particle Data Group, S. Eidelman *et al.*, Phys. Lett. B **592**, 1 (2004).

[13] BABAR Collaboration, B. Aubert *et al.*, hep-ex/0207070 ; Belle Collaboration, K. Abe *et al.*, hep-ex/0207098 .

[14] The Heavy Flavour Averaging Group, http://www.slac.stanford.edu/xorg/hfag/.

[15] Y. Grossman and M.P. Worah, Phys. Lett. B **395**, 241 (1997); Y. Grossman, G. Isidori and M.P. Worah, Phys. Rev. D **58**, 057504 (1998).

[16] J.C. Pati and A. Salam, Phys. Rev. D **10**, 275 (1974); R.N. Mohapatra and J.C. Pati, *ibid.* **11**, 566 (1975); **11**, 2558 (1975).

[17] M.A.B. Bég, R.V. Budny, R.N. Mohapatra, and A. Sirlin, Phys. Rev. Lett. **38**, 1252 (1977).

[18] For a review, see P. Langacker and S. U. Sankar, Phys. Rev. D **40**, 1569 (1989).

[19] DØ Collaboration, S. Abachi *et al.*, Phys. Rev. Lett. **76**, 3271 (1996).

[20] CDF Collaboration, F. Abe *et al.*, Phys. Rev. Lett. **74**, 2900 (1995).

[21] For a review, see R. N. Mohapatra, *Unification and Supersymmetry* (Springer, New York, 1992).

[22] P. Langacker, in *CP violation*, edited by C. Jarlskog (World Scientific, Singapore, 1989).

[23] T. Inami and C.S. Lim, Prog. Theor. Phys. **65**, 297 (1981).

[24] G. Beall, M. Bander, and A. Soni, Phys. Rev. Lett. **48**, 848 (1982).

[25] R.N. Mohapatra, G. Senjanović, and M.D. Tran, Phys. Rev. D **28**, 546 (1983); R. Decker and U. Türke, Z. Phys. C **26**, 117 (1984); G. Ecker and W. Grimus, *ibid.* **30**, 293 (1986); P. Ball, J.-M. Frère, and J. Matias, Nucl. Phys. **B572**, 3 (2000).

[26] G. Barenboim, J. Bernabeu, and M. Raidal, Phys. Rev. Lett. **80**, 4625 (1998); G. Barenboim, J. Bernabeu, J. Matias, and M. Raidal, Phys. Rev. D **60**, 016003 (1999); M. Raidal, Phys. Rev. Lett. **89**, 231803 (2002).

[27] P. Cho and M. Misiak, Phys. Rev. D **49**, 5894 (1994).

[28] R.N. Mohapatra and G. Senjanović, Phys. Rev. Lett. **44**, 912 (1980); Phys. Rev. D **23**, 165 (1981).

[29] B. Balke *et al.*, Phys. Rev. D **37**, 587 (1988).

[30] K. Fujikawa, B.W. Lee, and A.I. Sanda, Phys. Rev. D **6**, 2923 (1972)

[31] J. Chay, K.Y. Lee, and S.-h. Nam, Phys. Rev. D **61**, 035002 (1999); also see Ref. [21] .

[32] For a review, see J.J. Sakurai, *Currents and Mesons* (The University of Chicago Press, Chicago, 1969).

[33] D. Chang, J. Basecq, L.-F. Li, and P.B. Pal, Phys. Rev. D **30**, 1601 (1984).

[34] W.-S. Hou and A. Soni, Phys. Rev. D **32**, 163 (1985); J. Basecq, L.-F. Li, and P.B. Pal, *ibid.* **32**, 175 (1985).

[35] F.I. Olness and M.E. Ebel, Phys. Rev. D **30**, 1034 (1984); D. London and D. Wyler, Phys. Lett. B **232**, 503 (1989); also see Ref. [18].

[36] M.B. Voloshin, Mod. Phys. Lett. A **12**, 1823 (1997).

[37] M.K. Gaillard and B.W. Lee, Phys. Rev. D **10**, 897 (1974).

[38] C.W. Bernard *et al.*, Phys. Rev. Lett. **81**, 4812 (1998).

[39] G. Buchalla, A.J. Buras, and M. Lautenbacher, Rev. Mod. Phys. **68**, 1125 (1996); A.J. Buras, hep-ph/9806471 .

[40] M. Ciuchini *et al.*, Phys. Lett. B **316**, 127 (1993); Nucl. Phys. **B415**, 403 (1994); also see Ref. [39] .

[41] G. Ecker and W. Grimus, Nucl. Phys. **B258**, 328 (1985).

[42] R. Fleischer, Z. Phys. C **58**, 483 (1993); *ibid.* **62**, 81 (1994).

[43] M. Bauer, B. Stech, and M. Wirbel, Z. Phys. C **29**, 637 (1985); *ibid.* **34**, 103 (1987); A. Ali and C. Greub, Phys. Rev. D **57**, 2996 (1998).

[44] N.G. Deshpande and J. Trampetic, Phys. Rev. D **41**, 2926 (1990); H. Simma and D. Wyler, Phys. Lett. B **272**, 395 (1991).

[45] A. Ali, G. Kramer, and C.-D. Lü, Phys. Rev. D **59**, 014005 (1998).

[46] BABAR Collaboration, B. Aubert *et al.*, Phys. Rev. D **65**, 051101 (2002).